Use of Membranes in Gas Conditioning

Hope Baumgarner

Chelsea Ryden

Professor Dr. Miguel Bagajewicz

8 May 2009

Executive Summary

Natural gas processing is one of the largest industrial gas separation applications worldwide and is on the verge of innovative technology which may prove more economically sound. One such technology is membrane networks which compete directly with amine units to separate carbon dioxide from natural gas. Currently, membrane networks consisting of multiple membranes, compressors, mixers and splitters are being investigated to determine whether these systems can handle larger flow rates than membrane units at a reduced cost.

A model was designed in GAMS to assess the feasibility of an amine unit versus a membrane network where the annual processing cost was minimized. Several membrane networks processing natural gas at 19% CO_2 were designed to determine the optimal network. The two membrane network resulted in an annual processing cost of $163K with a total of 11% methane lost. A four membrane network was run in GAMS resulting in the three membrane network which was the optimal solution. The three membrane network had the smallest annual processing cost of $130K with 7.77% methane lost. Furthermore, the three membrane network was scaled up at varying flow rates with 19% and 9% CO_2 to compare the operating cost and total annualized cost to the amine unit's. At flow rates less than 270 MMscfd (19% CO_2) the membrane network had lower operating costs ranging from $175K to $39MM and a total annualized cost ranging from $202K to $45MM. At the same flow rates, the amine unit had operating costs ranging from $490K to $37MM and a total annualized cost ranging from $532K to $38MM. For the 9% CO_2 case, the membrane network had a lower operating cost of $16MM and a total annualized cost of $17MM at a flow rate below 150MMscfd. At the same flow rate and CO_2 concentration, the amine unit's operating cost and total annualized cost were $16.5MM and $17.5MM. It is recommended that membrane networks be used in applications with high CO_2 concentrations at flow rates less than 270 MMscfd.

Table of Contents

1. Introduction

Roughly 550 trillion scf (standard cubic feet) of natural gas in the lower 48 states cannot be processed because of high CO_2 content. Membrane networks for gas conditioning have the potential to process this low quality natural gas. Carbon dioxide, which is an acid gas, is commonly found in natural gas streams at levels as high as 50%. It is corrosive which rapidly destroys pipelines unless it is removed. Some common techniques for acid gas removal include absorption processes, cryogenic processes, adsorption processes and membrane separation. Membrane gas separation techniques were first introduced in the 1980's, and since then membrane based gas separation has developed into a $150 million per year business (Kookos, 193). Membranes are increasingly being used in applications which have larger flow rates and high CO_2 content.

The total worldwide consumption of natural gas is roughly 95 trillion scf/yr. The increased consumption of natural gas is the driver for innovative technology due to the high cost of equipment which is roughly $5 billion per year. However, membranes have less than five percent of this market (Baker, 2109). This paper summarizes current natural gas processing, membrane theory, optimization of membrane networks and a cost analysis between an amine unit and a three membrane network.

2. Natural Gas Processing

Current natural gas processing techniques require a number of steps prior to consumer usage. Although raw natural gas is primarily composed of methane, other impurities such as hydrogen sulfide, carbon dioxide, nitrogen, water vapor and helium are also present. Moreover, raw natural gas is commonly mixed with hydrocarbons such as ethane, propane, and butane which are valuable by products when separated. Prior to the distribution of natural gas, it must be processed to meet federal regulations which specify the composition of the sale gas. According to these pipeline regulations, the sale gas must contain less than 2% carbon dioxide and trace amounts of water vapor, hydrogen sulfide, nitrogen and other hydrocarbons. These stringent guidelines are aimed at reducing pollutant emissions as well as reducing the amount of corrosive components like carbon dioxide and hydrogen sulfide from damaging pipe lines.

The series of steps involved in natural gas processing consist of oil and condensate removal, acid gas removal, dehydration, nitrogen rejection, natural gas liquid separation, and fractionation. In order to transport and process natural gas, the oil in which it is dissolved in has to be removed. This typically takes place at or near the well head. In some instances, the separation of natural gas and oil will occur on its own during production due to decreased pressure. In this case, a conventional separator uses the force of gravity to separate the natural gas from the oil. However, sometimes specialized equipment such as a low temperature separator is used to remove any oil from the natural gas. This piece of equipment uses pressure differentials throughout different sections of the separator creating temperature variation. As a result, oil and some water vapor are condensed out of the wet gas stream. Once this separation is achieved, the raw natural gas is sent to an acid gas removal unit also known as an amine unit. Here the natural gas which contains relatively high levels of carbon dioxide and hydrogen sulfide is treated with an amine solution. As the sour gas runs through the tower, carbon dioxide and sulfur are removed because of the amine solution’s affinity for the two. The most commonly used amine solutions are monoethanolamine (MEA) and diethanolamine (DEA). Typically, the sulfur which was removed from the sour gas is sent to a Claus unit where it is converted into elemental sulfur. After the natural gas has been sweetened, it is sent to a dehydration unit to remove the existing water vapor using either adsorption or absorption. During absorption a drying agent such as diethylene glycol or triethylene glycol comes into contact with the wet natural gas removing the water vapor. Adsorption differs from absorption because a solid desiccant which also promotes drying is used to collect the water vapor from the wet gas onto its surface. Next, nitrogen is removed from the natural gas using a cryogenic, adsorption, or absorption process. During cryogenic expansion, the temperature of the gas stream is dropped to around -120 °F using a turbo expander. This allows some components in the gas stream to condense while leaving methane in a gaseous state. Prior to the sale of natural gas, the natural gas liquids must be removed using either a cryogenic expansion process or absorption process. Once the natural gas liquids have been recovered from the gas stream, they are sent to a fractionation unit in order to separate the by-product into its individual constituents such as ethane, propane, and butane. The technology used in natural gas processing has not seen much change in the past few decades; however, advances in natural gas production may prove beneficial to this industry.

3. Membrane Theory

A membrane separation process is used to separate a feed mixture containing two or more species through the use of a semi-permeable barrier where one species moves faster than the

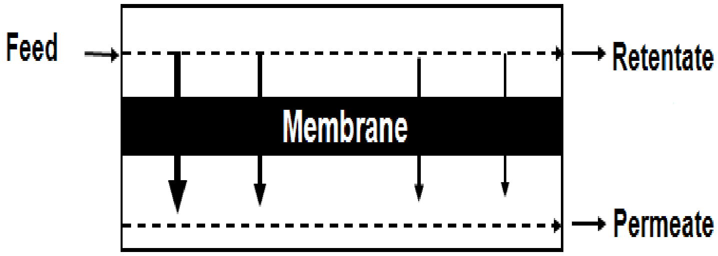

Figure 1. Basic membrane model (Sikavitsas)

other. Figure 1 depicts the most general membrane separation process in which the feed is separated into a retentate and permeate. The retentate is termed the slow gas as it does not pass through the membrane while the permeate is termed the fast gas as it passes through the membrane. The following membrane theory was referenced from Seader and Henley.

Mass transport through membranes is described by Fick's Law

$$N_i = \frac{D_i}{l_m}(c_{io} - c_{iL}) \tag{1}$$

where N_i is the molar flux of species i, D_i is the diffusivity of component i, l_m is the membrane thickness, c_{io} is the concentration of component i at the feed membrane interface and c_{iL} is the concentration of component i at the permeate membrane interface (see Figure 2). However, Fick's Law is not valid at the interface. Therefore, thermodynamic equilibrium is assumed so that Fick's Law can be related to the partial pressures through Henry's Law

$$H_{io} = {}^{c_{io}}/_{p_{io}} \tag{2}$$

$$H_{iL} = {}^{c_{iL}}/_{p_{iL}} \tag{3}$$

where the subscripts o and L refer to the feed membrane interface and membrane permeate interface, respectively, c_i is the concentration of component i, p_i is the partial pressure of component i and H_i is solubility constant.

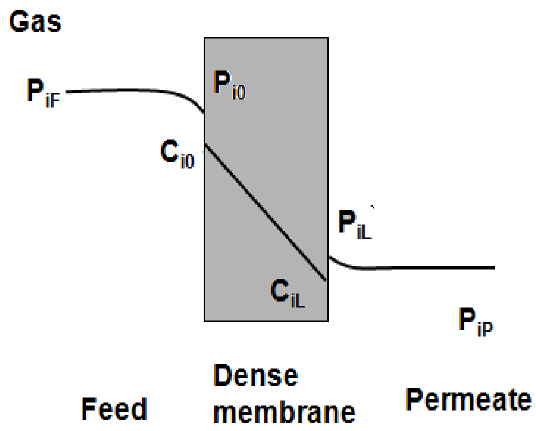

Figure 2. Membrane concentration profile (Sikavitsas)

Assuming H_i is independent of the total pressure and that the temperatures at both interfaces are the same, then

$$H_{io} = H_{iL} = H_i \tag{4}$$

Combining equations (1), (2) and (4)

$$N_i = \frac{H_i D_i}{l_m}(p_{io} - p_{iL}) \tag{5}$$

Neglecting external mass transfer resistances

$$p_{iF} = p_{io} \tag{6}$$

$$p_{iL} = p_{iP} \tag{7}$$

where each variable is shown in Figure 2.

Substituting equations (6) and (7) into (5) gives

$$N_i = \frac{H_i D_i}{l_m}(p_{iF} - p_{iP}) = \frac{P_{Mi}}{l_M}(p_{iF} - p_{iP}) \tag{8}$$

where

$$P_{Mi} = H_i D_i \tag{9}$$

where P_{Mi} is the permeability and P_{Mi}/l_M is the permeance.

A high flux can be achieved with a thin membrane and a high feed side pressure. Therefore, an ideal membrane would have a high permeance and also a high separation factor α (also known as selectivity).

$$\alpha_{A,B} = \frac{(y_A/x_A)}{(y_B/x_{\boldsymbol{B}})} \tag{10}$$

where A and B represent components, y_i is the mole fraction in the permeate and x_i is the mole fraction in the retentate. For a binary gas mixture

$$N_A = \frac{H_A D_A}{l_M}(x_A P_F - y_A P_P) \tag{11}$$

$$N_B = \frac{H_B D_B}{l_M}(x_B P_F - y_B P_P) \tag{12}$$

where P_F is the feed side pressure and P_P is the permeate side pressure. The ratio of N_A to N_B can then be described by the ratio of y_A to y_B

$$\frac{N_A}{N_B} = \frac{y_A}{y_B} = \frac{H_A D_A}{H_B D_B}\frac{(x_A P_F - y_A P_P)}{(x_B P_F - y_B P_P)} \tag{13}$$

If the feed side pressure is much greater than the permeate side pressure the following results.

$$\frac{N_A}{N_B} = \frac{y_A}{y_B} = \frac{H_A D_A}{H_B D_B}\frac{(x_A P_F)}{(x_B P_F)} = \frac{H_A D_A x_A}{H_B D_B x_B} \tag{14}$$

Rearranging equation (14) and substituting in equation (9) yields the ideal separation factor.

$$\alpha_{A,B} = \frac{(y_A/x_A)}{(y_B/x_B)} = \frac{H_A D_A}{H_B D_B} = \frac{P_{M_A}}{P_{M_B}} \tag{15}$$

Therefore, the selectivity is the ratio of the component's permeabilities.

4. Membrane Modules

Membrane for gas permeation can be found in one of the following modules: hollow fiber or spiral wound. Both types of membrane modules are produced and neither one has been deemed better than the other. Table 1 is a comparison of the characteristics of these two modules.

Table 1. Comparison of membrane modules (Seader, 502)

	Spiral-Wound	Hollow-Fiber
Packing Density, m^2/m^3	200-800	500-9,000
Resistance to fouling	Moderate	Poor
Ease of cleaning	Fair	Poor
Relative cost	Moderate	Low
Main applications	D, RO, GP, UF, MF	D, RO, GP, UF

D=Dialysis, RO=Reverse Osmosis, GP=Gas Permeation, PV=Pervaporation, UF=Ultrafiltration, MF=Microfiltration

4.1 Spiral-Wound

Spiral wound modules are the least common modules which compose less than 20% of membranes formed (Baker, 1395). Although they have a higher production cost ($10-100/m^2), this is compensated for by their high permeance and flux (Baker, 1395). Another advantage of spiral wound modules is their ability to use a wide range of materials compared to hollow fiber modules. Lastly, spiral wound modules are more resistant to plasticization, resulting in a longer life span.

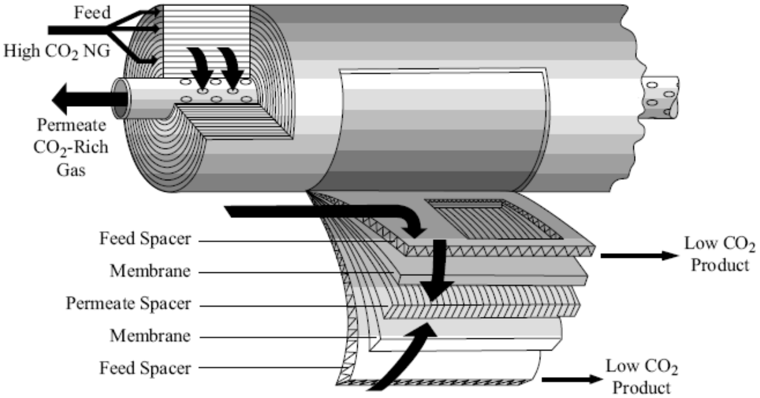

Figure 3. Spiral wound membrane module (Dortmundt, 7)

4.2 Hollow-Fiber

Hollow fiber membranes are the most common type of module. Hollow fiber modules have a greater packing density, i.e., more membrane area per unit volume, than spiral wound modules. Hollow fiber modules have a higher packing density because fine fibers can be used in the module, therefore allowing more fibers and thus a higher packing density. As a result, hollow fiber plants are typically smaller than spiral wound plants. Also, hollow fiber membranes tend to have a lower flux than spiral wound membranes because the layer through which the gas permeates is thicker.

The low cost (\$2-5/m^2) of hollow fiber modules makes it advantageous over spiral wound modules (Baker, 1395). Although the low cost of hollow fiber modules might be appealing, membrane modules only make up about 10-25% of the total plant cost (Baker, 1395). Therefore, reductions in the membrane module cost may not significantly reduce the overall plant cost.

Lastly, hollow fiber membranes have the selectivities and flux required. The major problem is the low reliability of these membranes caused by fouling. Moreover, hollow fiber modules require more careful and expensive treatment to avoid these problems.

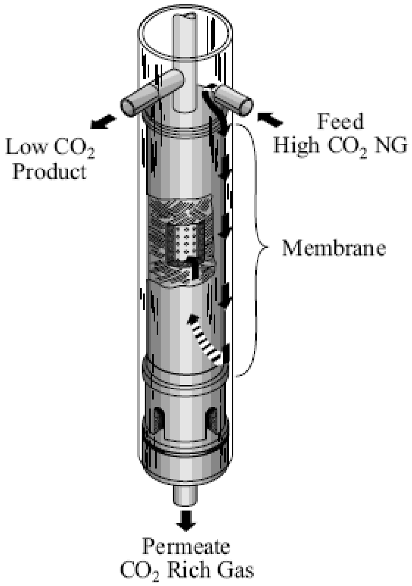

Figure 4. Hollow fiber membrane module (Dortmundt, 8)

5. Commercially Available Membrane Material

Although several types of materials used in membranes exist, it is essential that the material used be appropriate for the application. Some parameters to consider when selecting an appropriate material are selectivity, cost, and durability. In general, the major cost factor in membrane networks is not the material. In the case of natural gas processing, the membrane material must be able to withstand the operating conditions. For example, the material of interest should be able to remain stable in the presence of components such as benzene, toluene, ethybenzene, and xylene. Even though it is not typical for membrane networks to operate under substantially high flow rates compared to current natural gas processing units, the material's performance should not be hindered by varying conditions such as temperature, pressure and gas composition.

A membrane material's degree of selectivity is crucial for adequate separation to occur. A common membrane material used in industry is known as cellulose acetate. One of the reasons it is favored in industry is because it has a high selectivity for carbon dioxide over methane, and it is stable in the presence of most organic solvents. Membrane materials used for natural gas processing are classified according to the type of polymer in which they are constructed from. In the case of cellulose acetate, the polymer which comprises this material is known as a glassy polymer. The structure of a glassy polymer is rigid and tough because it is below the glass transition temperature. As a result, the polymer chains have limited mobility causing the membrane to discriminate between molecules based on size. Furthermore, polymers above their glass transition point are termed rubbery polymers. Some examples of commercially available rubbery polymers are silicone rubber and amide block co-polymers. Rubbery polymers differ from glassy polymers in that the polymer chains are more mobile and the material is more elastic. This difference allows membranes composed of rubbery polymers to separate components based on condensability. Condensability is the ease at which a gas is able to transition from a gaseous state to a liquid state onto the surface of the membrane material allowing it to be collected separately. In order to determine the type of polymer which is best suited to separate a desired component from a gas mixture, it is vital to evaluate the physical properties of the polymer. For example, glassy polymers are typically used to separate carbon dioxide from methane because they separate based on size. However, rubbery polymers can be used when one component condenses more readily than another which is the case for the separation between hydrogen sulfide and carbon dioxide. The properties of the membrane material are crucial in determining its performance, degree of selectivity, cost and durability.

6. Investigated Membrane Material

Cellulose acetate is one of the most common polymers used in membrane material for natural gas processing, but compared to other investigated material its selectivity for hydrogen sulfide over methane is inferior. Some examples of new polymeric membranes include polydimethylsiloxane, pebax, poly(ether/ester urethane), poly(sulfone), and poly(butadiene). These polymeric membranes have been studied for the purpose of acid gas applications and based on some experimental results have a significantly higher selectivity for hydrogen sulfide compared to cellulose acetate. In a study conducted to determine the permeation behavior of CO_2, H_2S and CH_4 in poly (ester urethane urea), selectivities of 43 and 16 were measured for H_2S/CH_4 and CO_2/CH_4 (Mohammadi 7361). At the same experimental conditions, the selectivities for H_2S/CH_4 and CO_2/CH_4 in cellulose acetate were 22 and 19 (Mohammadi 7361). These results demonstrate the potential for polymeric membranes in acid gas removal, but some draw backs such as plasticization and thermal stability have postponed further implementation. Plasticization occurs when the polymer within the membrane begins to swell due to the sorption of carbon dioxide. This decreased performance causes the membrane to lose its selectivity properties. These issues have accelerated further investigation into plasticization resistant material. Based on recent studies, silver incorporated pebax was shown to be resistant to plasticization and its measured selectivities for CO_2/CH_4 and H_2S/CH_4 were 13 and 50 (Sridhar 8144). The addition of silver to pebax enhanced some of its properties such as its diffusive selectivity which favors the transport of CO_2. Moreover, this material demonstrated hydrophilic behavior and was able to remove water vapor in the gas mixture at a relatively rapid rate. Other issues with polymeric membranes are the two opposing effects of high feed pressures on the permeation rate inside the membrane. The increased feed pressure can increase the free volume available, thus increasing the permeation rate. However, increased feed pressure also provokes membrane compression which decreases the free volume and decreases the permeation rate. Recent studies have been conducted to address these issues and with further exploration into these limitations solutions are bound to arise.

7. Membrane Advantages

High Concentration Gas

Membrane plants are more efficient at treating high concentration gas streams than lower concentration gas streams. A membrane plant designed to treat 5 million scfd of gas that contains 20% carbon dioxide would be less than half the size of a membrane plant designed to treat 20 million scfd of gas that contains 5% carbon dioxide (Baker, 2113).

Small Gas Flow

Membrane plants have simple flow schemes, which make them preferable when processing small gas flows. Also, membrane plants which are processed at lower flow rates of less than 20 million scfd of gas are designed so that operators are not needed (Baker, 2113).

Lower Capital Cost

Membrane systems are housed in skids. Skid mounted membrane plants allow for more area to be packed into a smaller volume as shown in Figure 5. Therefore minimal cost and time

Figure 5. A CO_2 membrane separation plant. This is a 9 million scfd membrane plant designed to reduce a 6% CO_2 gas to 2%. (Baker, 2113)

are necessary to prepare the site. Moreover, installation costs are significantly lower than those for alternative technologies.

Operational simplicity

Single stage membrane systems are very simple to operate because they require minimal downtime. If upsets do not occur, they are able to operate unattended for a significant amount of time. While single stage membranes do not require staffing, multiple stage membrane systems only require a minimal amount. Multiple stage membrane functions, such as start up, operation and shutdown, can be easily controlled from a control room.

Space efficiency

Figure 6 displays the space efficiency of skids. Membrane units can be assembled into compact modules, resulting in minimal space requirements. Membrane skids are advantageous and very common on offshore environments where space efficiency is necessary.

Figure 6. The skid in the lower left replaced all the units to the right (Dortmundt, 25)

Design Efficiency

Dehydration and CO_2 and H_2S removal are integrated into one operation in membrane systems. In traditional CO_2 removal technologies, these operations are performed in multiple stages.

Reduced Power & Consumption

Membrane systems greatly reduce the electric power and fuel consumption compared to conventional separation techniques.

Eco-friendly

Membrane systems are environmentally friendly as the permeate gases can be re-injected into the well or used as fuel.

8. Membrane Disadvantages

Plasticization

Membrane materials absorb 30-50 cm^3 of CO_2/cm^3 polymer. This results in a sharp drop in the polymer glass transition temperature and therefore a decrease in selectivity (Baker, 2114).

Physical Aging

The glassy polymers are in a non equilibrium state and over time the polymer chains relax, resulting in a decrease in permeability (Baker, 2114).

High Skid Cost

The cost of the membrane is a small fraction of the total skid cost. The membrane module cost often only makes up about 10-25% of the total cost (Kookos, 193). Moreover, reductions in membrane cost may not significantly change the total plant cost. Skid costs are high because of the large required compressor power. One way to lower the membrane skid cost is to increase the permeance of the membrane. This allows a smaller membrane area to be used to treat the same volume of gas. Another way to lower the membrane skid cost is to increase the feed gas pressure. As a result, the area and skid size is reduced. Consequently, this increases the energy consumption as larger compressors are necessary.

9. Membrane Applications

Within the past fifty years, membrane technology has been used in a myriad of applications such as reverse osmosis, gas separation, and alcohol dehydration. It was in the mid 1960's that a common membrane material today, cellulose acetate, was used to desalinize saltwater to produce drinkable water with less than 500 ppm of solids (Seader, 493). Later in 1979, Monsanto Chemical Company used hollow-fiber membranes comprised of polysulfone to enrich streams containing hydrogen and carbon dioxide (Seader, 493). Furthermore, the commercialization of alcohol dehydration led to the use of membrane technology as well as the need to remove metals and organics from waste water (Seader, 493). Although membrane networks have been used in a variety of fashions, one of the more pertinent applications has been its introduction into natural gas processing.

Due to the high volume of natural gas consumed worldwide, ~95 trillion scf/yr, natural gas processing is one of the largest industrial gas separation applications (Baker, 2109). Membrane processes make up less than five percent of natural gas processing equipment. One of the primary reasons membrane processes are used in natural gas processing is for carbon dioxide removal. Therefore, membrane technology competes directly with amine units which are primarily used to remove corrosive components such as carbon dioxide and hydrogen sulfide. Amine units are well received in the natural gas processing industry; however, many limitations such as high maintenance issues and well monitored operating procedures restrict the use of amine treatment units in remote locations. In the 1980's, the use of membrane networks for carbon dioxide removal became appealing in remote areas where constant monitoring was not available. Some of the first companies to operate a membrane system to separate carbon dioxide from natural gas were Grace Membrane Systems, Separex, and Cynara (Baker, 2110). At this time, one of the most commonly used polymers was cellulose acetate, but within the past ten years other membrane materials such as polyimide polymers and perfluoropolymers have challenged its use. Recent advancements in membrane technology have made its implementation more attractive, but this technology remains limited.

10. Amine Unit

As mentioned before, amine treatment units are typically used to remove corrosive components in natural gas namely carbon dioxide and hydrogen sulfide. The details of this process will be discussed in order to provide a comprehensive view of this unit. Moreover, the inner workings of the amine treatment unit are necessary to understand the assessment of this unit with the investigated membrane network. A typical process flow through an amine treatment unit can be seen in Figure 7. First, the sour gas enters an inlet separator which removes any liquids or solids present in the gas mixture. Once the sour gas leaves the inlet contactor it enters the bottom of the contactor where it contacts an amine solution. During this contact, components in the acid gas react with the amine solution to form a salt. The gas continues to move up the column and the sweetened gas exits at the top of the column where it passes through an outlet separator. Next, the sweetened gas must go through dehydration to remove the excess water. The sweetened gas also goes through a water wash in order to recover any vaporized and entrained amine solution. The rich amine solution exiting the contactor enters a flash drum to remove the remaining hydrocarbons. After leaving the flash drum, the rich amine solution passes through an exchanger where it absorbs heat. This heated amine solution flows into the mid section of the stripper where hydrogen sulfide and carbon dioxide are removed. Once this is completed, the lean solution leaves the bottom of the stripper and passes through the rich/lean exchanger and then to a lean cooler. The lean solution is cooled down to a temperature that is about 10 °F warmer than the inlet gas to the contactor to remain above the hydrocarbon dew point. Finally, the lean solution returns to the contactor to repeat the cycle.

The acid gas that is stripped from the amine solution exits the top of the stripper where it passes through a condenser and separator to cool the stream and recover water which is returned to the stripper as reflux. It is common for the acid gas leaving the stripper to be vented, incinerated, sent to a Claus unit, compressed for sale, or re-injected into a reservoir for oil recovery (Engineering Data Book 21-9). This approach for acid gas removal is widely used in industry because it is provides adequate CO_2 and H_2S separation at a relatively low cost. However, at smaller flow rates this method may not be the most economically feasible and will be assessed in subsequent sections of this report.

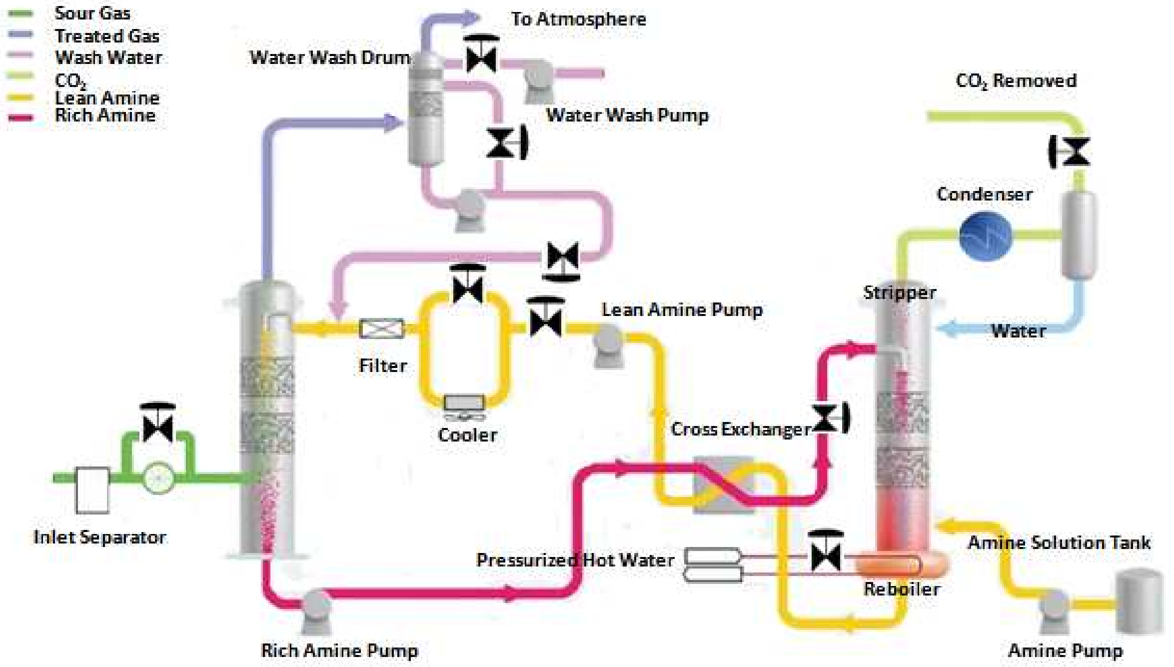

Figure 7. Amine unit process flow diagram

11. Development of Model

11.1 Comparison between GAMS and Excel results

The initial step in modeling countercurrent flow in the membrane network was to perform a single membrane simulation in a program called GAMS. GAMS is a general algebraic modeling system which allows the user to set up a series of sets, parameters, equations and bounds in order to minimize or maximize a function of interest. A basic membrane simulation was created in GAMS with the equations shown in Table 2 and Figure 8 displays the variables and the membrane orientation. A more detailed description of these equations is presented in subsequent sections.

Table 2. Single membrane simulation equations

Flux Through Membrane	$dJ_{k,j,m} = Q_{m,j}(x^t_{k,j,m}P^t_m - x^s_{k+1,j,m}P^s_m)$
Shell Side Component Balance	$f^s_{k,j,m} = f^s_{k-1,j,m} + dJ_{k,j,m}dA$
Tube Side Component Balance	$f^t_{k,j,m} = f^t_{k+1,j,m} - dJ_{k,j,m}dA$
Shell Side Component Mole Fraction	$x^s_{k,j,m} = \frac{f^s_{k,j,m}}{\Sigma_j f^s_{k,m}}$
Tube Side Component Mole Fraction	$x^t_{k,j,m} = \frac{f^t_{k,j,m}}{\Sigma_j f^t_{k,m}}$
Total Flow Shell Side	$TFS_{k,m} = \Sigma_j f^s_{k,m}$
Total Flow Tube Side	$TFT_{k,m} = \Sigma_j f^t_{k,m}$

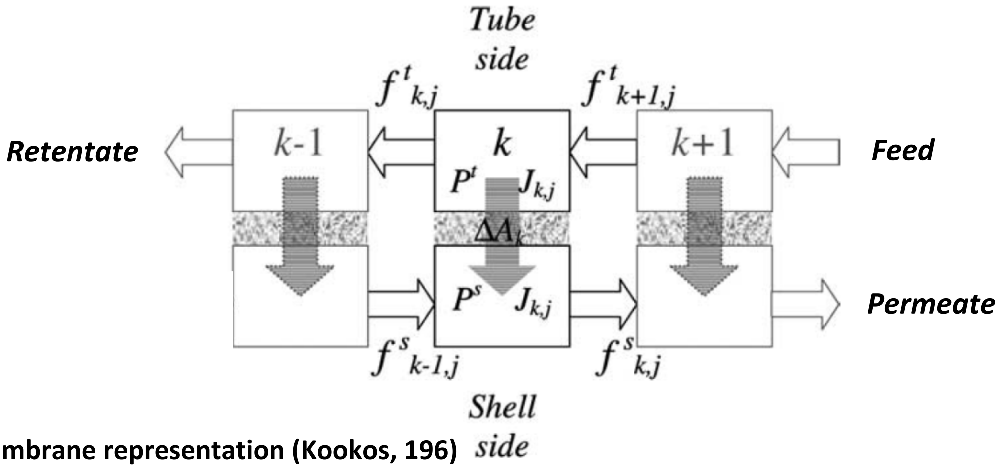

Figure 8. Membrane representation (Kookos, 196)

The following graph was produced from the simulation results.

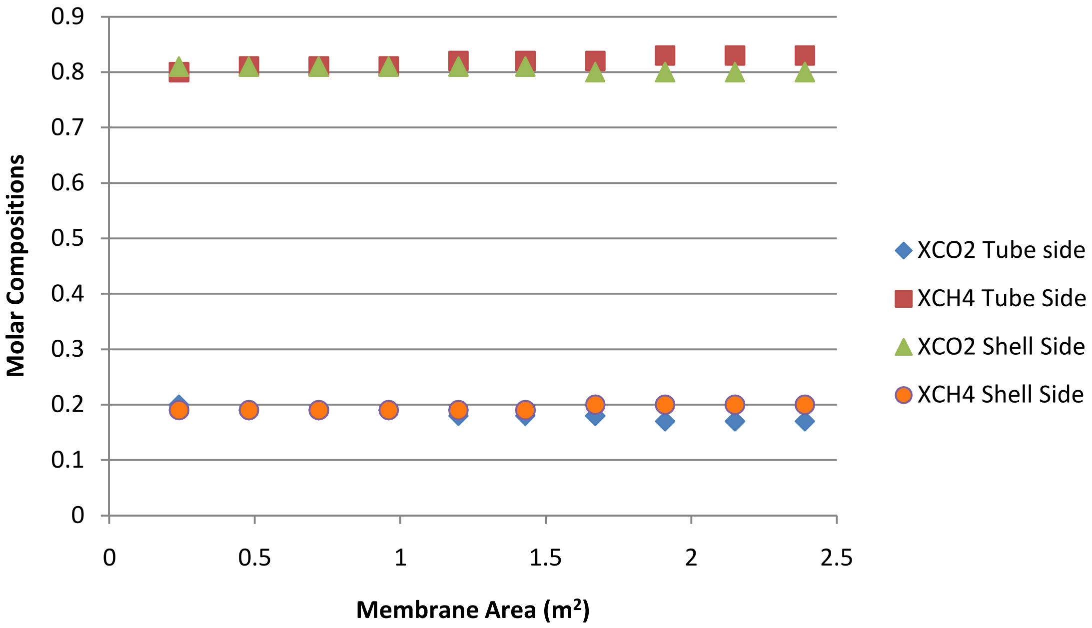

Figure 9. GAMS membrane simulation results

As expected the molar composition of CO_2 will decrease along the tube side as the CO_2 permeates through the membrane to the shell side. As the CO_2 composition decreases on the tube side, the composition of CH_4 will increase. These results are supported in Figure 9.

The equations from Table 2 were then implemented into Excel to verify the GAMS results. The following graphs produced from the Excel simulation also confirm the validity of the GAMS simulation. A comparison of membrane concentration profiles were constructed ranging from compositions of 0.9 CH_4 and 0.1 CO_2 to 0.5 CH_4 and 0.5 CO_2 for both the tube and shell side.

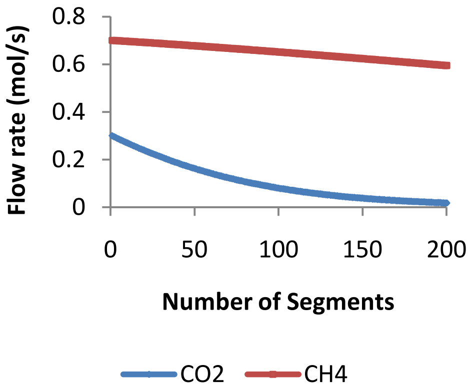

Figure 10. Excel simulation tube side 0.7 CH_4 & 0.3 CO_2

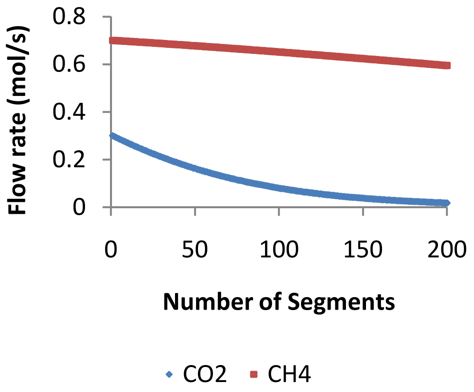

Figure 11. GAMS simulation tube side 0.7 CH_4 & 0.3 CO_2

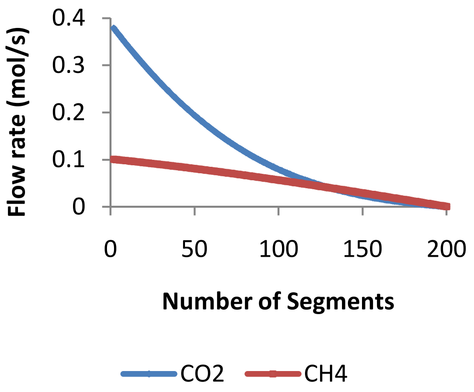

Figure 12. Excel simulation shell side 0.6 CH_4 & 0.4 CO_2

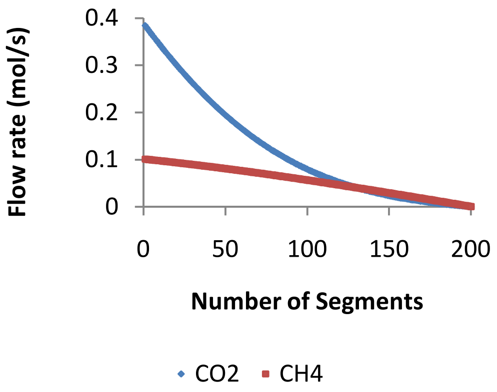

Figure 13. GAMS simulation shell side 0.6 CH_4 & 0.4 CO_2

Similar concentrations profiles between Excel and GAMS were also observed for the remaining three concentrations mentioned above. Therefore, it can be assured the equations are correct when implemented into the GAMS membrane network simulation.

11.2 Membrane Simulation Model

The objective function of interest for this model is aimed at minimizing the annual process cost which will be described later on in this section. The mathematical model used to describe the hollow fiber membrane simulation was based from a paper written by Ionannis K.

Kookos. The following equations for counter current flow are valid under the assumption that each segment has uniform properties, the gas is ideal, the process is at steady-state and is isothermal, and there is no pressure drop across the permeate side (Kookos, 196). Furthermore, the permeabilities of each component are considered constant and independent of concentration and diffusion does not occur in the axial direction (Kookos, 196). Also, this model does not take the deformation of the membrane fibers into consideration. The equations below describe how the membrane is modeled in GAMS as well as Excel.

Flux Through a Membrane

$$dJ_{k,j,m} = Q_{\boldsymbol{m,j}}(x^{t}_{k,j,m}P^{t}_{m} - \boldsymbol{x}^{s}_{k+1,j,m}P^{s}_{m}) \qquad . \tag{16}$$

Where $dJ_{k,j,m}$ is the flux of component j at a given segment for membrane m and $Q_{\boldsymbol{m,j}}$ is the permeability of component j and is dependent on the membrane material. This value is set as a parameter and was obtained for each of the components in cellulose acetate from literature. Moreover, $x^{t}_{k,j,m}$ is the mole fraction of component j on the tube side at a given segment, P^{t}_{m} is the tube side pressure for membrane m, $\boldsymbol{x}^{s}_{k+1,j,m}$ is the mole fraction on the shell side at the previous segment k+1, and P^{s}_{m} is the pressure on the shell side for membrane m. The pressures on the tube and shell side for this program are also set as parameters and were obtained from literature. The membrane is split into segments which are denoted by k because evaluating the membrane as a whole may yield erroneous results, and this approach has a simpler mathematical basis.

Shell Side Component Balance

$$f^{s}_{k,j,m} = f^{s}_{k-1,j,m} + dJ_{k,j,m}dA \tag{17}$$

Where $f^{s}_{k,j,m}$ denotes the flow of component j on the shell side at a given segment, $f^{s}_{k-1,j,m}$ is the flow of a component j on the shell side at the previous segment, and dA is the active area of the membrane.

Tube Side Component Balance

$$f^{t}_{k,j,m} = f^{t}_{k+1,j,m} - dJ_{k,j,m}dA \tag{18}$$

The above equation is essentially the same as equation (16), but deals with the flow on the tube side. Moreover, the feed to the membrane is on the tube side; therefore, as flow travels across the membrane a portion of this flow is lost to the shell side which is indicated by the (-) in this equation.

Shell Side Component Mole Fraction

$$x^{s}_{k,j,m} = \frac{f^{s}_{k,j,m}}{\sum_j f^{s}_{k,m}} \tag{19}$$

Where $x^{s}_{k,j,m}$ is the mole fraction on the shell side and is described as the quotient of component j's flow rate to the total flow rate on the shell side.

Tube Side Component Mole Fraction

$$x^{t}_{k,j,m} = \frac{f^{t}_{k,j,m}}{\sum_j f^{t}_{k,m}} \tag{20}$$

The above equation described is essentially the same as equation (19), but applies to the tube side.

Total Flow Shell Side

$$TFS_{k,m} = \sum_j f^{s}_{k,m} \tag{21}$$

Where $TFS_{k,m}$ is the total flow on the shell side across all segments and membranes and is the sum of all component flow rates across all segments and membranes.

Total Flow Tube Side

$$TFT_{k,m} = \sum_j f^t_{k,m} \tag{22}$$

This equation is the same as equation (21), but applies to flow on the tube side.

Based on the program, there are several versions of the transport equation and component mass balance equation on the tube and shell side. The overall equations which are described above are the same, but there are upper and lower bounds that are specified. These constraints (M) allow the program to search for a result that is either above or below the given constraint. The constant which is selected is arbitrary, but must be large or small enough so that the left hand side of the equation does not reach this value. It is essential that the user understand the overall program in order to properly specify these constants.

11.3 Mixer and splitter balances

Feed Balance

$$F_j = \sum_m fm_{j,m} \tag{23}$$

Where F_j denotes the feed flow rate of component j and $fm_{j,m}$ is the flow rate of component j to membrane m from the feed.

Feed Proportion

$$F_j \sum_l fm_{l,m} = fm_{j,m} \sum_l F_l \tag{24}$$

Where $fm_{l,m}$ is the total flow rate to membrane m from the feed and F_l is the total feed flow rate.

Retentate Balance

$$\sum_k retentateout_{k,j,m} = \sum_{ma} frm_{j,m,ma} + frout_{j,m} \tag{25}$$

Where $frm_{j,m,ma}$ denotes the retentate flow rate of component j from membrane m to ma and $frout_{j,m}$ is the retentate flow rate of component j from membrane m.

Retentate Composition

$$\sum_k retentateout_{k,j,m} = rc_{j,m} \sum_{k,l} retentateout_{k,l,m} \tag{26}$$

Where $rc_{j,m}$ denotes the retentate composition of component j from membrane m and $retentateout_{k,l,m}$ is the total retentate flow rate of segment k from membrane m.

Retentate to Membrane Proportion

$$frm_{j,m,ma} = rc_{j,m} \sum_l frm_{l,m,ma} \tag{27}$$

Where $frm_{l,m,ma}$ denotes the total retentate flow rate.

Permeate Balance

$$permeateout_{j,m} = \sum_{ma} fpm_{j,m,ma} + fpout_{j,m} \tag{28}$$

Where $fpm_{j,m,ma}$ denotes the permeate flow rate of component j from membrane m to ma and $fpout_{j,m}$ is the permeate flow rate of component j leaving membrane m.

Permeate Composition

$$pc_{j,m} = xs_{CO_2,j,m} \tag{29}$$

Where $pc_{j,m}$ denotes the permeate composition of component j from membrane m and $xs_{1,j,m}$ is the shell side mole fraction in segment 1 for component j of membrane m. Segment 1 is used because it is the last segment the gas travels through before exiting on the shell side.

CO$_2$ Composition

$$outr_{CO_2} \leq rcomp \sum_l outr_l \tag{30}$$

Where $outr_{CO_2}$is the flow rate of CO$_2$ in the retentate stream, $rcomp$ is 0.02 and $outr_l$ is the total flow rate of the retentate stream.

Permeate to Membrane Proportion

$$fpm_{j,m,ma} = pc_{j,m} \sum_l fpm_{l,m,ma} \tag{31}$$

Where $fpm_{l,m,ma}$ denotes the total permeate flow rate from membrane m to ma.

Mixer to Membrane

$$ftin_{j,m} = fm_{j,m} + \sum_{ma} frm_{j,ma,m} + \sum_{ma} fpm_{j,ma,m} \tag{32}$$

Where $ftin_{j,m}$ is the flow rate of component j to membrane m.

Total Retentate Out

$$outr_j = \sum_m frout_{j,m} \tag{33}$$

Where $outr_j$ is the final retentate flow rate of component j.

Retentate Out Proportion

$$frout_{j,m} = rc_{j,m} \sum_l frout_{l,m} \tag{34}$$

Where $frout_{l,m}$ is the total retentate flow rate from membrane m.

Total Permeate Out

$$outp_j = \sum_m fpout_{j,m} \tag{35}$$

Where $outp_j$ is the final permeate flow rate of component j.

Permeate Out Proportion

$$fpout_{j,m} = pc_{j,m} \sum_l fpout_{l,m} \tag{36}$$

Where $fpout_{l,m}$ is the total permeate flow rate leaving membrane m.

Compressor Power

Retentate Power

$$Wrm_{m,ma} = \left(\sum_j frm_{j,m,ma}\right)\left(\frac{n}{n+1}\right)\frac{Z_{in}+Z_{out}}{2}\frac{1}{\eta_a}RT_{in}\left[\left(\frac{Pt_{ma}}{Ps_m}\right)^{\frac{n-1}{n}} - 1\right] \tag{37}$$

Where $Wrm_{m,ma}$ is the work needed in the retentate stream from membrane m to ma, n is Cp/Cv where Cp is the heat capacity at constant pressure and Cv is the heat capacity at constant volume, Z_{in} is the inlet compressibility factor, Z_{out} is the outlet compressibility factor, η_a is the compressor efficiency, R is the gas constant, T_{in} is the inlet temperature, Pt_{ma} is the tube side pressure in membrane ma and Pt_m is the tube side pressure in membrane m.

Permeate Power

$$Wpm_{m,ma} = \left(\sum_j fpm_{j,m,ma}\right)\left(\frac{n}{n+1}\right)\frac{Z_{in}+Z_{out}}{2}\frac{1}{\eta_a}RT_{in}\left[\left(\frac{Pt_{ma}}{Ps_m}\right)^{\frac{n-1}{n}} - 1\right] \tag{38}$$

Where $Wpm_{m,ma}$ is the work needed in the permeate stream from membrane m to ma and Ps_m is the shell side pressure in membrane m.

Feed Power

$$Wfm_m = \left(\sum_j fm_{j,m,}\right)\left(\frac{n}{n+1}\right)\frac{Z_{in}+Z_{out}}{2}\frac{1}{\eta_a}RT_{in}\left[\left(\frac{Pt_m}{P_{feed}}\right)^{\frac{n-1}{n}} - 1\right] \tag{39}$$

Where Wfm_m is the work needed in the feed stream to membrane m and $Pfeed$ is the pressure of the feed.

11.4 Objective Function

In order to design an optimal membrane system, the annual process cost should include the capital investment associated with permeators and compressors as well as membrane maintenance, utility cost and product loss (Henson, 75). Moreover, the fixed capital investment associated with this membrane design includes the cost of the membrane housing; however, the replacement cost of the membrane components is considered an operating expense. Included in the membrane housing is the cost of pipes, fittings, and assembly (Henson, 76).

Annual Process Cost

$$F = F_{cc} + F_{mr} + F_{mt} + F_{ut} + F_{pl} \tag{40}$$

The annual product cost is the sum of the capital charge, membrane replacement cost, maintenance cost, utility cost, and cost due to product loss. Where F_{cc} is the capital charge

(USD/yr), F_{mr} is membrane replacement cost in (USD/yr), F_{mt} is membrane maintenance cost in (USD/yr), F_{ut} is utility cost in (USD/yr), and F_{pl} is the cost due to product loss in the permeate (USD/yr).

Fixed Capital Investment

$$F_{fc} = f_{mh} \sum Area + f_{cp} \frac{W_{cp}}{\eta_{CP}} \tag{41}$$

The fixed capital investment F_{fc} is a function of the membrane area and the compressor power. Where f_{mh} is the cost of the membrane housing which is estimated at \$200/m^2, f_{cp} is the cost of a gas powered compressor which is estimated at \$1000/KW, W_{cp} is the work of the compressor and η_{CP} is the compressor efficiency which is estimated at 70% (Henson , 78).

Capital Charge

$$F_{cc} = f_{cc}(1 + f_{wk})F_{fc} \tag{42}$$

The capital charge is estimated by annualizing the fixed capital investment and the working capital, f_{wk}, is taken as 10% of the fixed capital investment. The capital charge f_{cc} is estimated at 27% (Henson, 78).

Membrane Replacement Cost

$$F_{mr} = \frac{f_{mr}}{t_m} \sum Area \tag{43}$$

The membrane replacement cost is determined by the cost to replace each membrane which is estimated at \$90/m^2, the membrane life which is estimated at 3 years and the total area required for the membrane network (Henson, 78).

Membrane Maintenance Cost

$$F_{mt} = f_{mt} F_{fc} \tag{44}$$

The membrane maintenance cost, f_{mt}, is taken as 5% of the fixed capital investment.

Utility Cost

$$F_{ut} = \frac{f_{sg} t_{wk}}{f_{hv} \eta_{cp}} \sum W_{cp} \tag{45}$$

The cost of utilities can be determined in a number of ways; however, for this membrane network gas powered compressors will be used resulting in the above equation. Where f_{sg} is the price of the sale gas which is estimated at \$35/Km^3, t_{wk} is the working time which is assumed 350 days/year, and f_{hv} is the sales gas gross heating value which is estimated at 43MJ/m^3 (Henson, 78).

Product Loss

$$F_{pl} = f_{sg} t_{wk} m_p \tag{46}$$

The product loss is a function of the price of the sale gas, the working time and the total flow rate, m_p, of methane in the permeate.

The objective function described above takes several cost factors into consideration such as initial capital investment, maintenance and replacement cost, utility cost and cost due to loss of methane in the permeate. Although other objective function could be implemented into the model, this one was deemed most appropriate and yielded sufficient results.

11.5 Discrete Method

The discrete method is used in this model in order to describe non linear equations in a linear fashion. This is accomplished by dividing the variables into many segments and setting upper and lower bounds on the discretized variables. Moreover, this method allows continuous variables to be defined as parameters throughout each of the designated segments. The discrete method was implemented into our program for the component material balance on the shell and tube side, component mole fractions on the shell and tube side, retentate and permeate flow from one membrane to the other, and the final retentate and permeate flow rates out of the membrane network. Below are some examples of how these equations were discretized.

Lower Bound Component Flow Rate Tube Side

$$ft(k,j,m) = G = sigT(k,m)dxt(d) - 100(1 - yt(k,j,d,m)) \tag{47}$$

$$\frac{ft}{sigT} \geq dxt(d) - M \tag{48}$$

Upper Bound Component Flow Rate Tube Side

$$ft(k,j,m) = L = sigT(k,m)dxt(d+1) + feed(j)\big(1 - yt(k,j,d,m)\big) \tag{49}$$

$$\frac{ft}{sigT} \leq dxt(d) + M \tag{50}$$

The actual equations represented in the GAMS model are (47) and (49), and their simplified versions are (48) and (50). The parameter $dxt(d)$ is known as the discrete variable in this model and is divided into many segments. In order to identify the segment interval, a binary variable, yt, is used to designate this location. The constant which is *100* or M in this case is referred to as a constraint because the left hand side of the equation must be greater than this value. The same concept applies to equations (49) and (50), but represents the upper bound. This ideology was applied to other equations in the model, but for the sake of brevity will not be discussed further.

12. Results

After assessing the two, three and four membrane networks, the three membrane network was deemed optimal. Below are results which indicate which networks achieved the least amount of methane lost, lowest utility cost, and lowest annual processing cost. In addition, the process flow diagrams for each case are shown later in this section and display the resulting mole fractions in the primary streams. The appendix displays more detailed process flow diagrams which provide the mole fractions for each stream in the membrane network. Using the three membrane network, a comparison between this system and an amine unit was performed at varying flow rates with 19% CO_2. The results for the 3 membrane network at 238 lb-mol/hr were scaled up to higher flow rates which were more comparable to industry. Based on these results, membrane networks have a lower total annualized cost at flow rates less than 270 MMscfd compared to amine units.

12.1 Comparison Between Various Membrane Networks

As Table 3 indicates, each simulation provided the overall process cost, area, compressor work and methane lost. Although the compressor work for the three membrane network is the highest of the three the overall annual processing cost was the lowest. This result is because the three membrane network has the lowest methane lost which is a factor in the annual process cost. Even though the area of the three membrane network is much higher than the area of the two membrane network, the cost of the membrane is not a major contributing factor in the annual processing cost.

Table 3. Comparison between two, three, and four membrane networks at 79 lbmol/hr

	Objective Function ($)	Area (m^2)	W_{cp} (KW)	% CH_4 Lost
2-Membrane Network	163,000	160	0.42	11.2
3-Membrane Network	130,000	435	80	7.77
4-Membrane Network	130,000	435	80	7.77

12.2 Assessment of Amine Unit to Membrane Network

The overall objective for this assessment was to determine in which instances the investigated membrane network is more economically feasible than an amine unit. The results indicate that the membrane network has a lower total annualized cost than the amine unit at flow rates less than 270 MMscfd at 19% CO_2. Furthermore, the operating cost for the membrane network is smaller than the amine unit's at flow rates less than 270 MMscfd. For the second case study using the Williams concentration at 9% CO_2, it was found that the membrane network had a lower total annualized cost at flow rates less than 150 MMscfd. The operating cost for the membrane network is also lower than the amine unit at this flow rate. The primary utility involved in the membrane network is the compressors. At lower flow rates, the work required for the compressors does not exceed the utilities for an amine unit. However, at higher flow rates the work increases dramatically causing the operating costs for the membrane network to exceed that of the amine unit. The utilities required for an amine unit consist of compressors, heat exchangers, reboilers, and condensers which result in an overall higher utility cost. In the case of lower flow rates, the membrane network has an overall smaller total annualized cost and operating cost.

Although much investigation has been done studying the economics of membrane units versus amine units, these case studies were concerned with determining how well a membrane network would improve these results. From Figure 16, the superimposed lines from case study 1 (19% CO_2) demonstrate at which flow rates and CO_2 concentrations membrane networks compete with amine units. These results indicate that membrane networks are capable of processing natural gas with high CO_2 concentration at higher flow rates than membrane units. Once this upper flow rate limit is reached, it is recommended that membrane networks be used in conjunction with amine units. Although membrane networks have much potential, existing limitations such as compressor work and membrane material have restricted its use in high flow rate applications.

Table 4. Economic analysis of an amine unit and a membrane network at 19% CO_2

	Flow rate (MMscfd)	FCI ($)	Operating Cost ($/yr)	TAC ($/yr) 15 yr.
Membrane	2	405,000	175,000	202,000
	90	31,000,000	13,000,000	15,000,000
	180	61,000,000	26,000,000	30,000,000
	270	92,000,000	39,000,000	45,000,000
	360	123,000,000	52,000,000	60,000,000
	455	153,000,000	65,000,000	75,000,000
	550	184,000,000	77,000,000	90,000,000
Amine	2	632,000	490,000	532,000
	90	3,700,000	21,000,000	21,000,000
	180	6,600,000	30,000,000	30,000,000
	270	9,200,000	37,000,000	38,000,000
	360	11,500,000	43,000,000	44,000,000
	455	14,000,000	49,000,000	50,000,000
	550	17,000,000	54,000,000	55,000,000

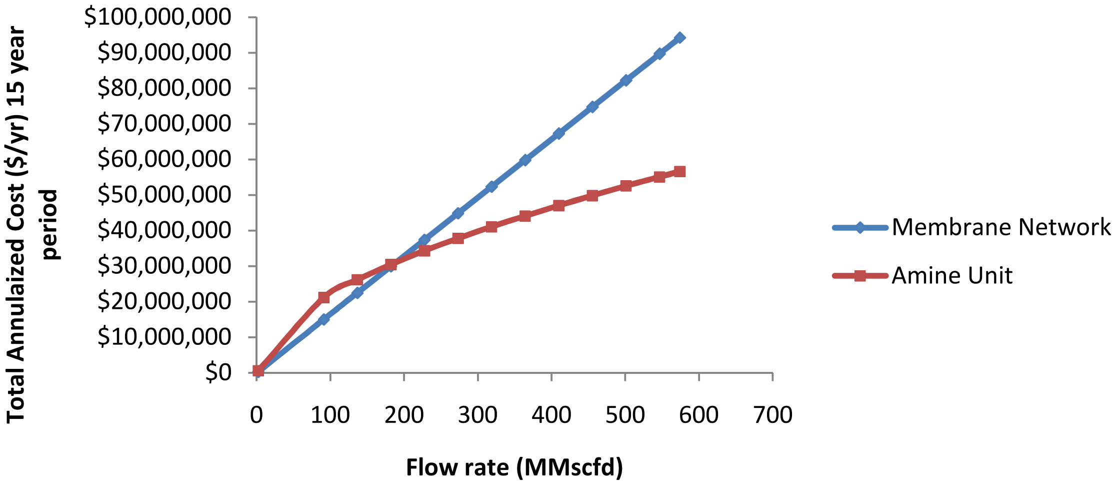

Figure 14. Total annualized cost versus flow rate for an amine unit and a membrane network at 19% CO_2

Table 5. Economic analysis of an amine unit and a membrane network at 9% CO_2

	Flow rate (MMscfd)	FCI ($)	Operating Cost ($/yr)	TAC ($/yr) 15 yr.
Membrane	90	18,000,000	9,000,000	10,000,000
	180	36,000,000	18,000,000	20,000,000
	270	55,000,000	27,000,000	31,000,000
	360	73,000,000	36,000,000	41,000,000
	455	91,000,000	45,000,000	51,000,000
	550	109,000,000	54,000,000	61,000,000
Amine	90	5,000,000	12,000,000	12,000,000
	180	6,000,000	17,000,000	18,000,000
	270	7,000,000	22,000,000	22,000,000
	360	8,000,000	26,000,000	26,000,000
	455	10,000,000	29,000,000	30,000,000
	550	11,000,000	33,000,000	33,000,000

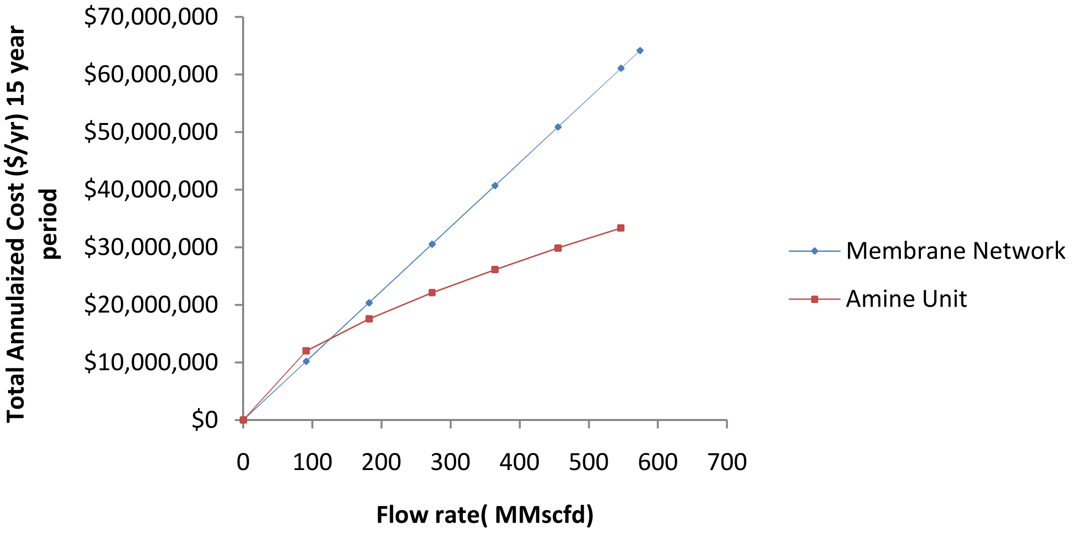

Figure 15. Total annualized cost versus flow rate for an amine unit and a membrane network at 9% CO_2

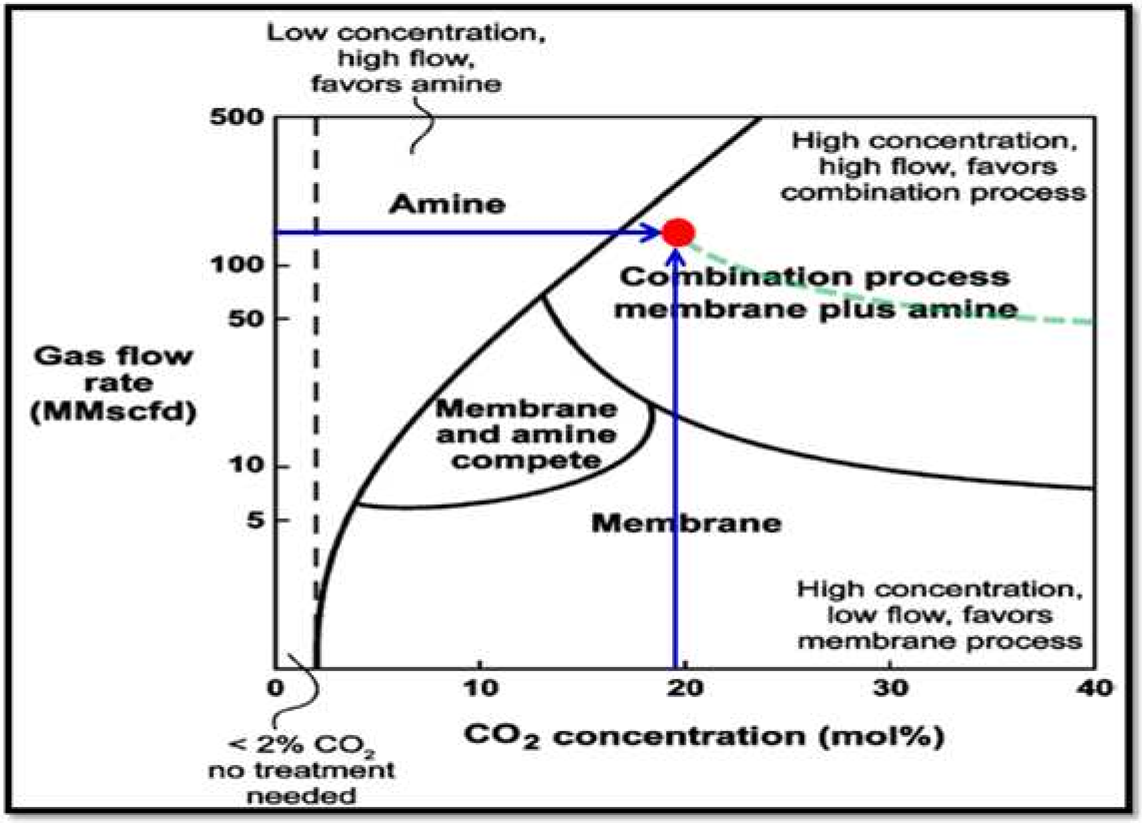

Figure 16. Existing cost comparison between an amine unit and a membrane unit

13. Recommendations

An optimum membrane network was determined to consist of three membranes. Membrane networks with flow rates lower than 270 MMscfd at 19% CO_2 and 150 MMscfd at 9% CO_2 have been recommended for CO_2 removal as opposed to an amine unit. However, membrane networks processing natural gas with lower CO_2 content do not compete as well with amine units at higher flow rates. Membrane networks are more useful in applications where natural gas containing high CO_2 concentrations must be processed. At higher CO_2 concentrations, membrane networks are able to compete with amine units at higher flow rates compared to applications with lower CO_2 concentrations. It is recommended that membrane networks be utilized at flow rates less than 270 MMscfd with 19% CO_2. Above these flow rates, membrane networks should be used in conjunction with an amine unit to remove CO_2.

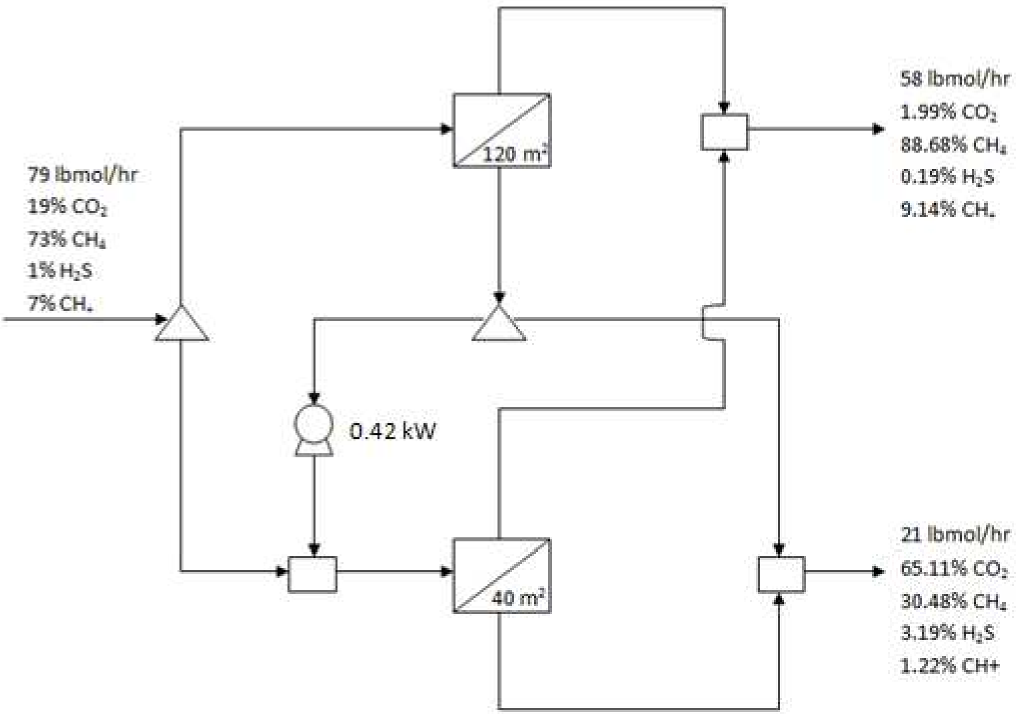

Figure 17. Two membrane network at 79 lb-mol/hr with 19% CO_2

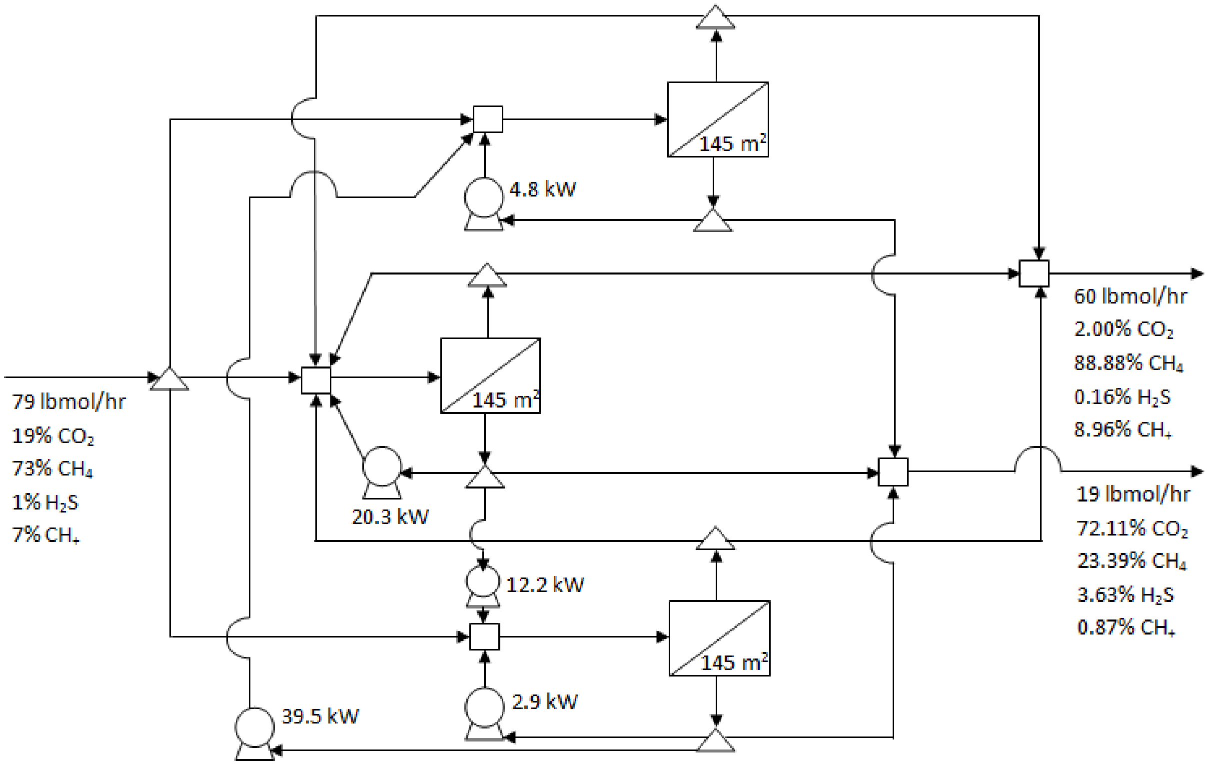

Figure 18. Three membrane network at 79 lb-mol/hr with 19% CO_2

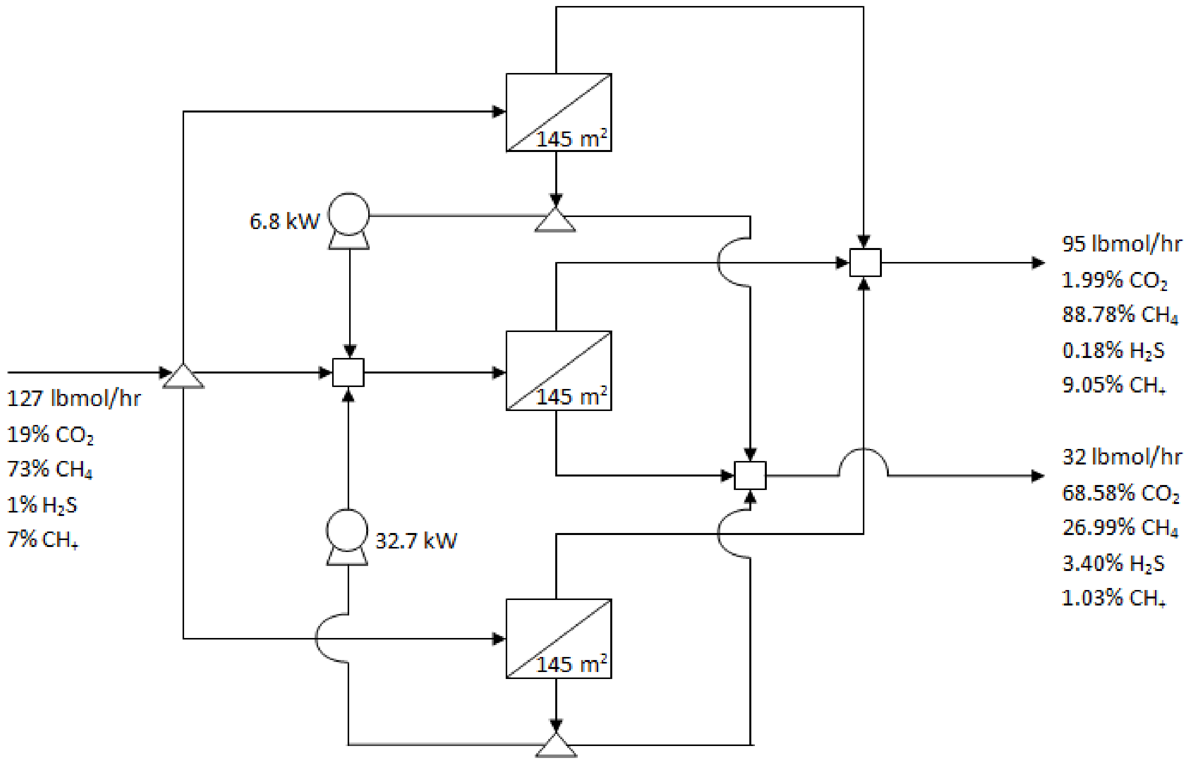

Figure 19. Three membrane network at 127 lb-mol/hr with 19% CO_2

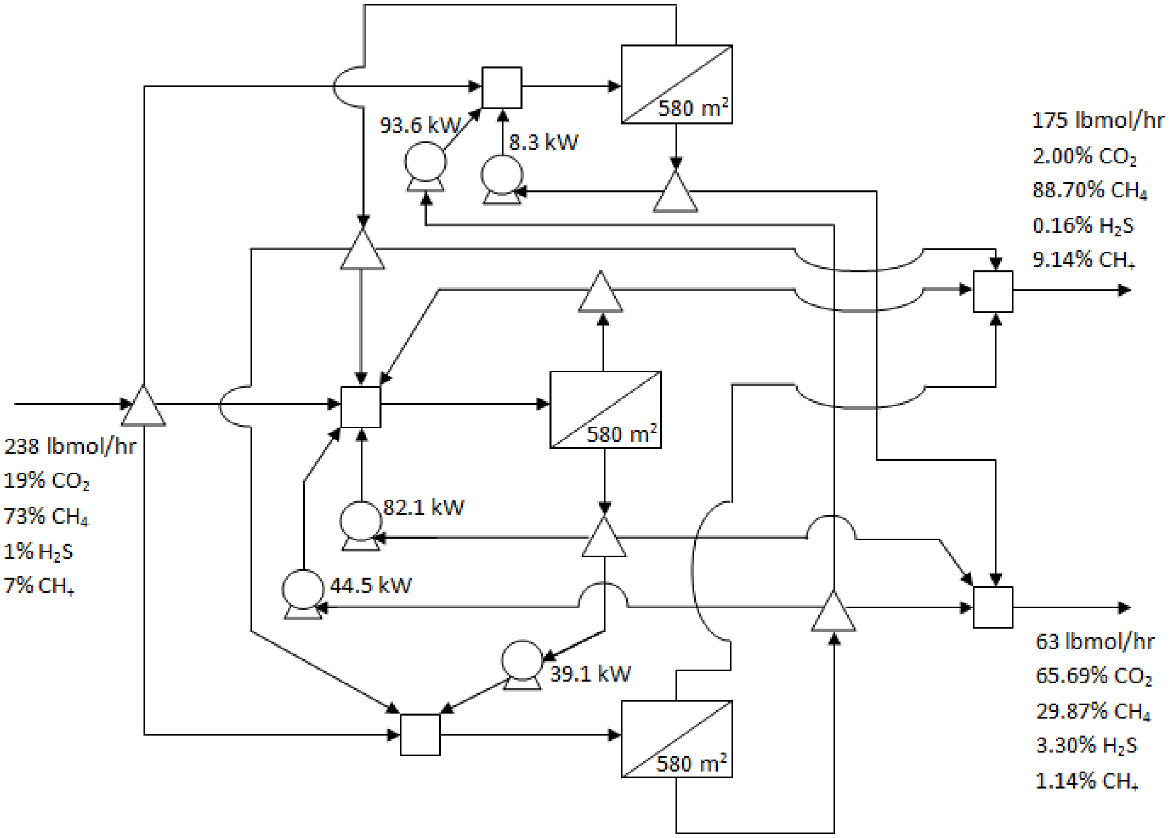

Figure 20. Three membrane network at 238 lb-mol/hr with 19% CO_2

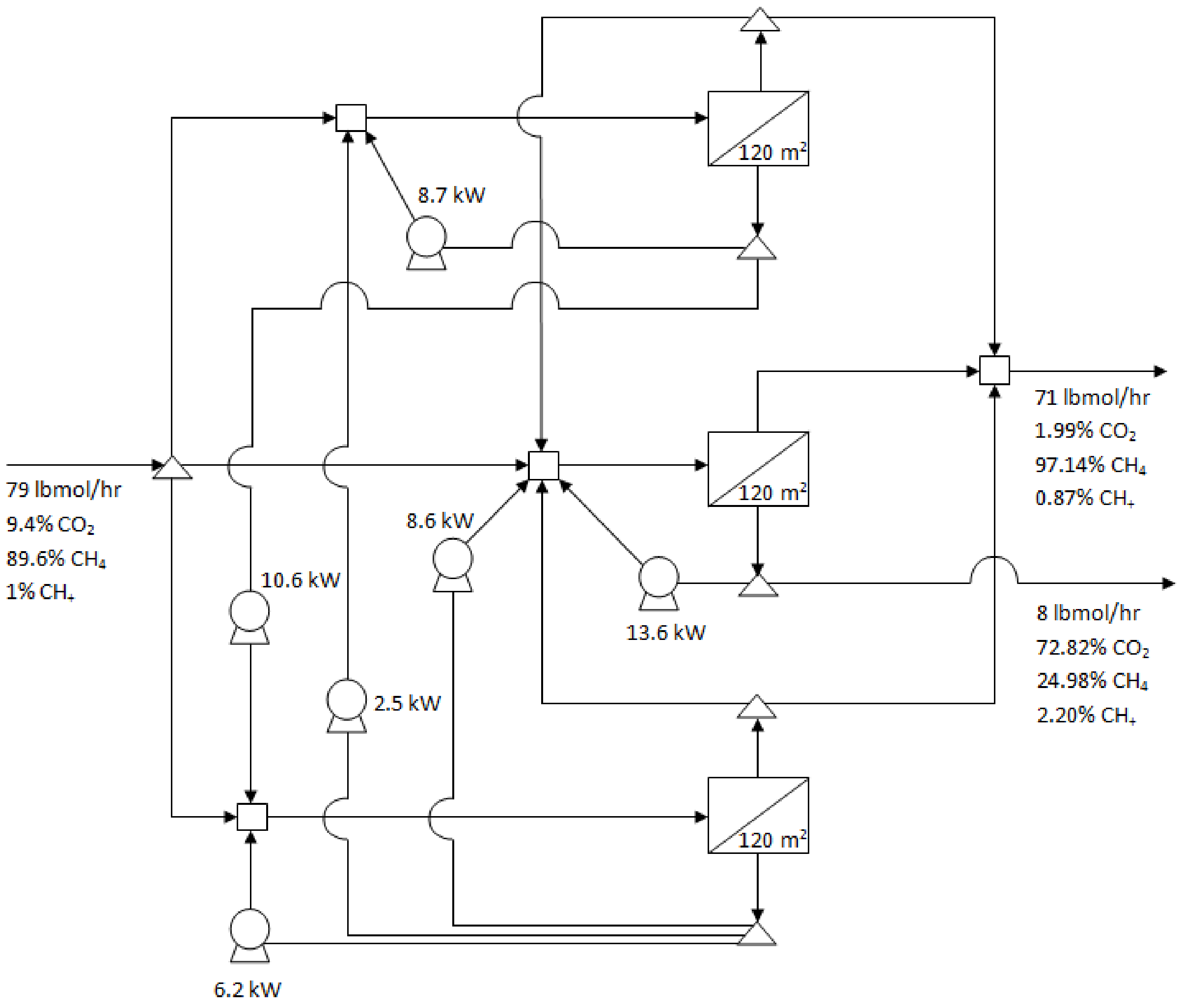

Figure 21. Three membrane network at 79 lb-mol/hr with 9% CO_2

References

Baker, Richard. “Future Directions of Membrane Gas Separation Technology.” *Industrial & Engineering Chemistry Research*. 2002. Sarkey’s Senior Lab. 7 Feb. 2009. <http://pubs.acs.org>.

Baker, Richard. Membrane Technology and Applications (2nd Edition). Wiley. 2004.

Baker, Richard and Kaaeid Lokhandwala. “Natural Gas Processing with Membranes: An Overview.” *Industrial & Engineering Chemistry Research.* 2008. Sarkey’s Senior Lab. 4 Feb. 2009 <http://pubs.acs.org>.

Dortmundt, David and Kishore Doshi. “Recent Developments in CO_2 Removal Membrane Technology.” *UOP LLC*. 1999. Sarkey’s Senior Lab. 7 Feb. 2009.

Engineering Data Book. (12th ed.). Gas Processors Supplies Association, Tulsa: 2004.

Faria, Debora C. “GAMS: Membrane Network Simulation.” *School of Chemical, Biological, and Materials Engineering*. January 2008.

Kookos, I.K. “A Targeting Approach to the Synthesis of Membrane Network for Gas Separations.” *Membrane Science*, p. 208, 193-202, 2002.

Li, N. Norman. Advanced Membrane Technology and Applications. Wiley. 2008.

Mohammadi, T., Moghadam, Tavakol, and et al. “Acid Gas Permeation Behavior Through Poly(Ester Urethane Urea) Membrane.”*Industrial & Engineering Chemistry Research.* 2008. Sarkey’s Senior Lab. 4 Feb. 2009 <http://pubs.acs.org>.

Natural Gas Supply Association. 2004. Sarkey’s Senior Lab. 7 Feb. 2009. <http://www.naturalgas.org/index.asp>.

Perry, R.H.; Green, D.W. (1997). Perry’s Chemical Engineers’ Handbook (7th Edition). McGraw-Hill.

Peters, Max S., Timmerhaus, Klaus D., & West, Ronald E. Plant Design and Economics for Engineers. (5th ed.). McGraw Hill, Boston: 2003.

Qi, R. and M. A. Henson, "Optimal design of spiral-wound membrane networks for gas separations.” *Journal of Membrane Science*, p. 75-78,1996.

Seader, J. D., and Henley, E. J. "Separation Process Principles.” New York: John Wiley & Sons, Inc., p. 718- 736, 1998.

Sridhar, S and et al. “Permeation of Carbon Dioxide and Methane Gases through Novel

Silver-Incorporated Thin Film Composite Pebax Membranes." *Industrial Engineering Chemistry Research* 2007 Sarkey's Senior Lab. 4 Feb 2009. <http://pubs.acs.org>

Appendix I

Sizing and Cost of an Amine Unit

In order to compare the equipment cost, fixed capital investment, working capital, total capital investment and the utility cost of an amine unit versus a membrane network, a simulation package known as Pro-II was used to develop an amine unit model. The program was able to give us information regarding the diameter and tray spacing for each distillation column, the overall heat transfer coefficient for each heat exchanger, pump capacity, and the heat duty for the distillation column. Based on these results, each piece of equipment was sized according to equipment pricing charts in <u>Plant Design and Economics for Chemical Engineers</u>.

Distillation Column

Once the simulation was completed, an estimated design value for the diameter and tray spacing for each column was reported. Based on the number of trays in the column which was chosen and the tray spacing, the height of each column can be determined. Using figure 15-11 from <u>Plant Design and Economics for Chemical Engineers</u>, the cost of the column can be estimated from the vertical height and diameter of the column. Moreover, materials other than carbon steel have adjustment factors which must be taken into consideration. However, carbon steel was used for the external material so this adjustment was not necessary. The estimated cost for the trays was found in figure 15-13 and is based on the column diameter as well as the type and material of the tray. For this application, valve trays were selected using stainless steel. Stainless steel was chosen because the trays will come into contact with an amine solution which is extremely corrosive. Also, a quantity factor is used to adjust the cost depending on the amount of trays used for each column.

Heat Exchanger & Valves

The information used to price the heat exchanger was the overall heat duty which was reported as the product of the heat exchanger area (UA Btu/hr-F). Using table 14-5 from Plant Design and Economics for Chemical Engineers, the overall heat transfer coefficient for each exchanger can be estimated based on the type of component passing through the exchanger. For example, some heat exchangers in the amine unit may contact light organics where as others contact water. Based on the design values for the overall heat transfer coefficient, the overall area required for the heat exchanger can be determined. From figure 14-17, the cost of the heat exchanger can be estimated based on the total area and the material. The material used for this application was carbon steel. The cost for the valves was found in figure 12-8 and stainless steel gate valves were selected for this design.

Pumps

The simulation in Pro-II provided the capacity or the flow rate at the inlet of the pump which is used to estimate the purchasing cost. From figure 12-21 in Plant Design and Economics for Chemical Engineers, the purchasing cost for the pump can be determined based on the pump capacity and the material used. Again carbon steel was used and a pressure adjustment factor of 1.1 was accounted for.

MDEA Calculations

In order to get an accurate equipment cost, the amount of MDEA needed for the initial start-up was calculated. This value was determined by finding the amount of hold-up on each of the trays in the contactor and the regenerator as well as the hold up in the pipes. Furthermore, with each cycle some MDEA is lost and must be replenished; thus this cost was also considered.

Note to reader

The tables below are for three different flow rates with 19% CO_2. However, flow rates ranging from 10,000-60,000 lb-mol/hr for both 9% and 19% CO_2 are detailed in an excel sheet.

Summary of Equipment and Utility Cost: 79 lb-mol/hr

Table 6. Equipment cost for an amine unit operating at 79 lb-mol/hr & 19% CO_2

Columns		Type	No. of trays	Operating pressure	Cost
1	Absorber	Valve trays	6	250 psia	$15,334
2	Stripper	Valve trays	12	16 psia	$32,736
Exchangers		MOC	Duty (MMBtu/hr)	Area (ft2)	
1	Rich amine / Lean amine	Stainless Steel	16.45	241.73955	$4,772
2	Lean amine / water	Stainless Steel	10.96	37.191652	$2,651
3	Lean amine / water	Stainless Steel	6.098	28.193677	$2,439
Pump		MOC	Power (HP)		
	Pump lean amine solution	Stainless Steel	130		$1,803
Valve		MOC	Diameter (m)	Type	
Rich amine expansion valve		Stainless Steel	0.2	Flanged	$8,484
MDEA initial amt cost					$552
Total					$68,771

Table 7. Utility cost for an amine unit operating at 79 lb-mol/hr & 19% CO_2

	Flow(1000 kg/hr)	Price ($ /m3)	Cost ($ / yr)
Cooling water	17.53959549	0.29	$42,726
Natural gas as heating utility for reboiler	Reboiler (MMBtu/hr)	Price ($ / MMBTU)	
	2.73	5	$114,516
Electricity	Duty (kW)	Price ($ / kWh)	
	4.42	0.062	$2,301.94
MDEA Recycle	Flow (lb/hr)	Price ($/lb)	
	0.11917	1.54	$1,541.58
Total			$161,086

Summary of Equipment and Utility Cost: 127 lb-mol/hr

Table 8. Equipment cost for an amine unit operating at 127 lb-mol/hr & 19% CO_2

	Columns	Type	No. of trays	Operating pressure	Cost
1	Absorber	Valve trays	6	250 psia	$15,424
2	Stripper	Valve trays	12	16 psia	$37,434
	Exchangers	MOC	Duty (MMBtu/hr)	Area (ft2)	
1	Rich amine / Lean amine	Stainless Steel	16.45	711.08872	$9,544
2	Lean amine / water	Stainless Steel	10.96	94.337643	$3,075
3	Lean amine / water	Stainless Steel	6.098	185.37014	$4,242
	Pump	MOC	Power (HP)		
	Pump lean amine solution	Stainless Steel	130		$1,909
	Valve	MOC	Diameter (m)	Type	
	Rich amine expansion valve	Stainless Steel	0.2	Flanged	$8,484
	MDEA initial amt cost				$701
	Total				$80,813

Table 9. Utility cost for an amine unit operating at 127 lb-mol/hr & 19% CO_2

Cooling water	Flow(1000 kg/hr)	Price ($ /m3)	Cost ($ / yr)
	44.80690133	0.29	$109,150
Natural gas as heating utility for reboiler	Reboiler (MMBtu/hr)	Price ($ / MMBTU)	
	6.96	5	$292,374
Electricity	Duty (kW)	Price ($ / kWh)	
	11.2611	0.062	$5,864.78
MDEA Recycle	Flow (lb/hr)	Price ($/lb)	
	0.11917	1.54	$1,541.58
Total			$408,930

Summary of Equipment and Utility Cost: 238 lb-mol/hr & 19% CO_2

Table 10. Equipment cost for an amine unit operating at 238 lb-mol/hr & 19% CO_2

Columns		Type	No. of trays	Operating pressure	Cost
1	Absorber	Valve trays	6	250 psia	$27,932
2	Stripper	Valve trays	12	16 psia	$53,235
Exchangers		MOC	Duty (MMBtu/hr)	Area (ft2)	
1	Rich amine / Lean amine	Stainless Steel	16.45	804.06735	$15,907
2	Lean amine / water	Stainless Steel	10.96	113.88082	$4,242
3	Lean amine / water	Stainless Steel	6.098	86.315086	$3,712
Pump		MOC	Power (HP)		
	Pump lean amine solution	Stainless Steel	130		$2,651
Valve		MOC	Diameter (m)	Type	
Rich amine expansion valve		Stainless Steel	0.2	Flanged	$8,484
MDEA initial amt cost					$871
Total					$117,033

Table 11. Utility cost for an amine unit operating at 238 lb-mol/hr & 19% CO_2

	Flow(1000 kg/hr)	Price ($ /m3)	Cost ($ / yr)
Cooling water	53.48166714	0.29	$130,281
Natural gas as heating utility for reboiler	Reboiler (MMBtu/hr)	Price ($ / MMBTU)	
	8.311611536	5	$349,088
Electricity	Duty (kW)	Price ($ / kWh)	
	13.62	0.062	$7,093.30
MDEA Recycle	Flow (lb/hr)	Price ($/lb)	
	0.23834	1.54	$3,083.17
Total			$489,545

Pro-II Verification

A Pro-II simulation was performed for all resulting membrane networks. This was done in order to verify the compressor work as it is a major contributing factor in the total cost. The Pro-II simulation for the 3 membrane network at 238 lb-mol/hr is shown in the following figure.

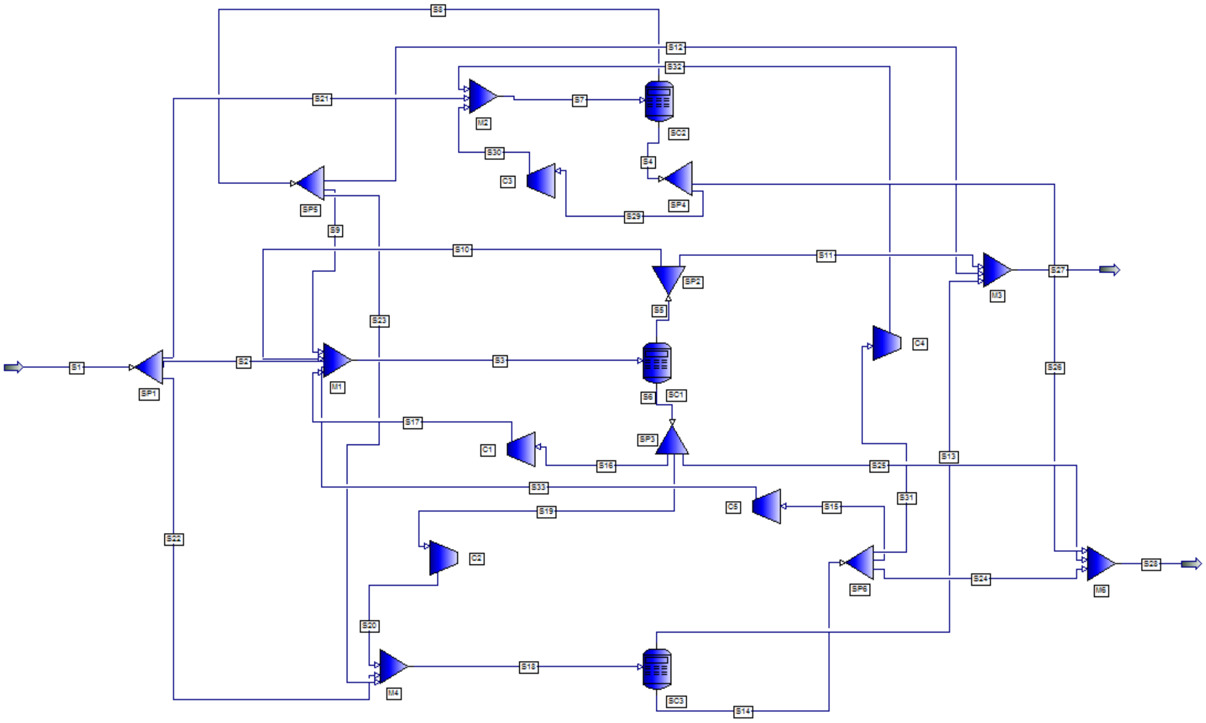

Figure 22. Membrane network simulation

The following table is a comparison of the compressor work found from our model and Pro-II.

Table 12. Compressor work comparison

Compressor	Model Work (kW)	Pro-II Work (kW)
C1	82.1	82.9
C2	39.1	39.5
C3	8.3	8.4
C4	93.6	94.7
C5	44.5	44.2

Amine Simulation

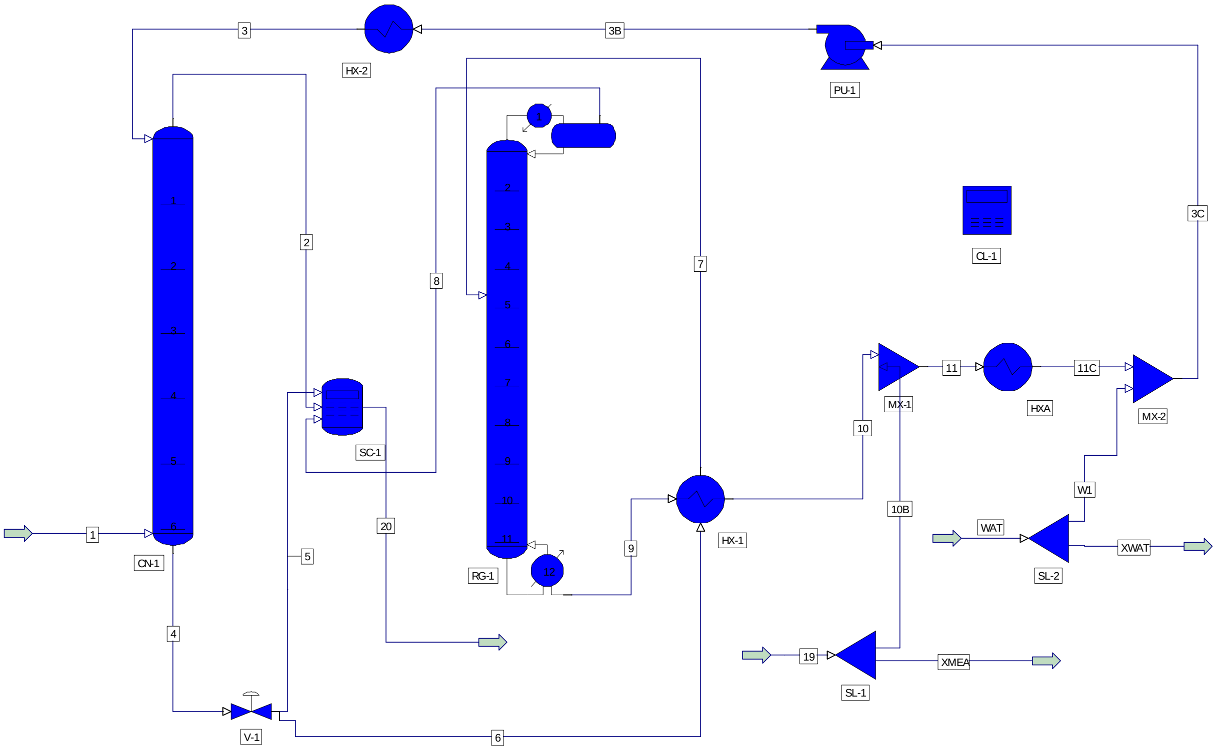

Figure 23. Amine unit simulation process flow diagram from Pro-II

Membrane Networks

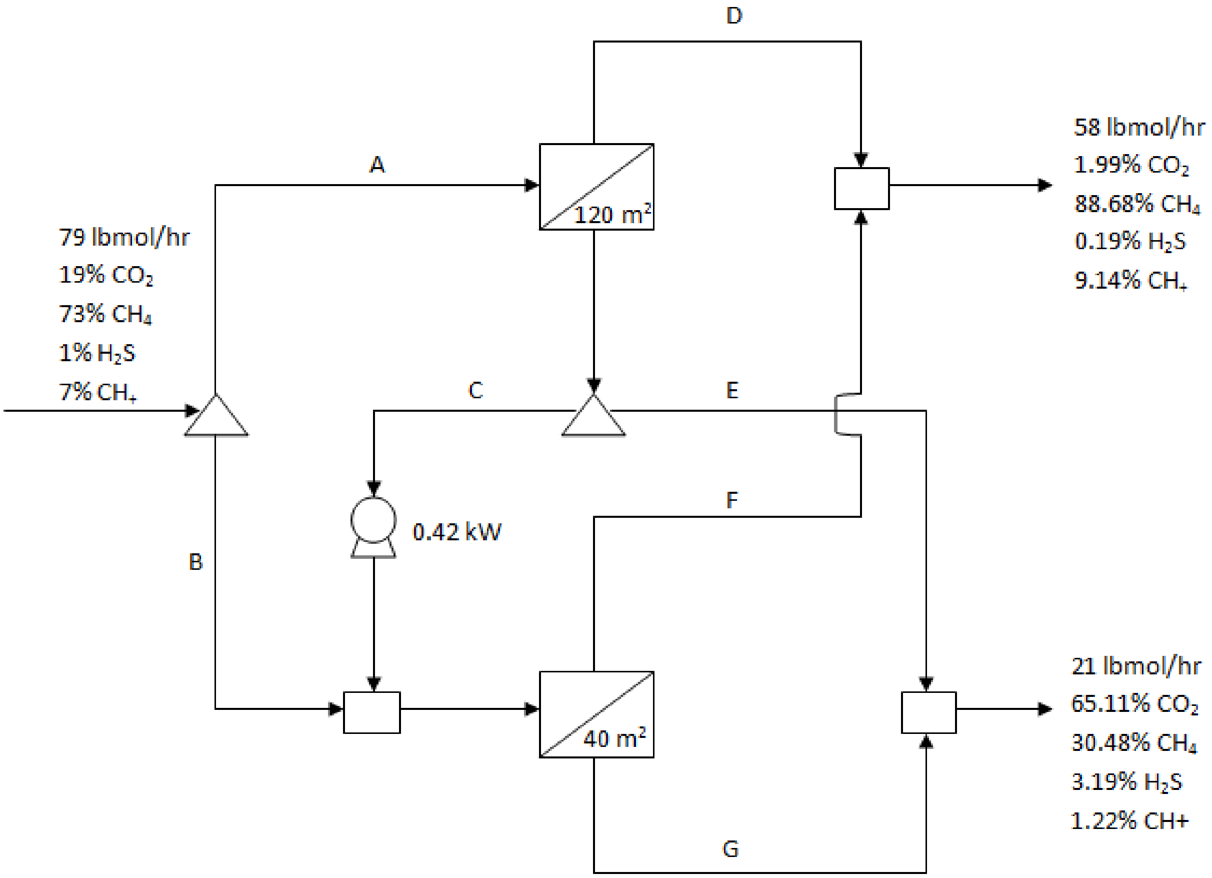

Figure 24. Two membrane network at 79 lb-mol/hr with 19% CO_2

Table 13. Two membrane network molar compositions at 79 lb-mol/hr with 19% CO_2

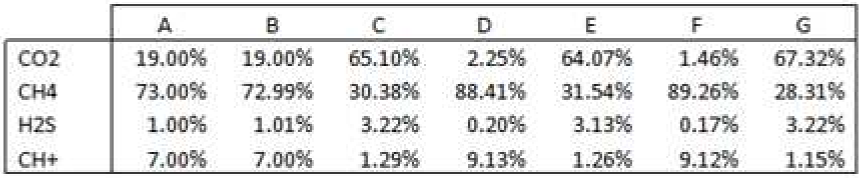

	A	B	C	D	E	F	G
CO2	19.00%	19.00%	65.10%	2.25%	64.07%	1.46%	67.32%
CH4	73.00%	72.99%	30.38%	88.41%	31.54%	89.26%	28.31%
H2S	1.00%	1.01%	3.22%	0.20%	3.13%	0.17%	3.22%
CH+	7.00%	7.00%	1.29%	9.13%	1.26%	9.12%	1.15%

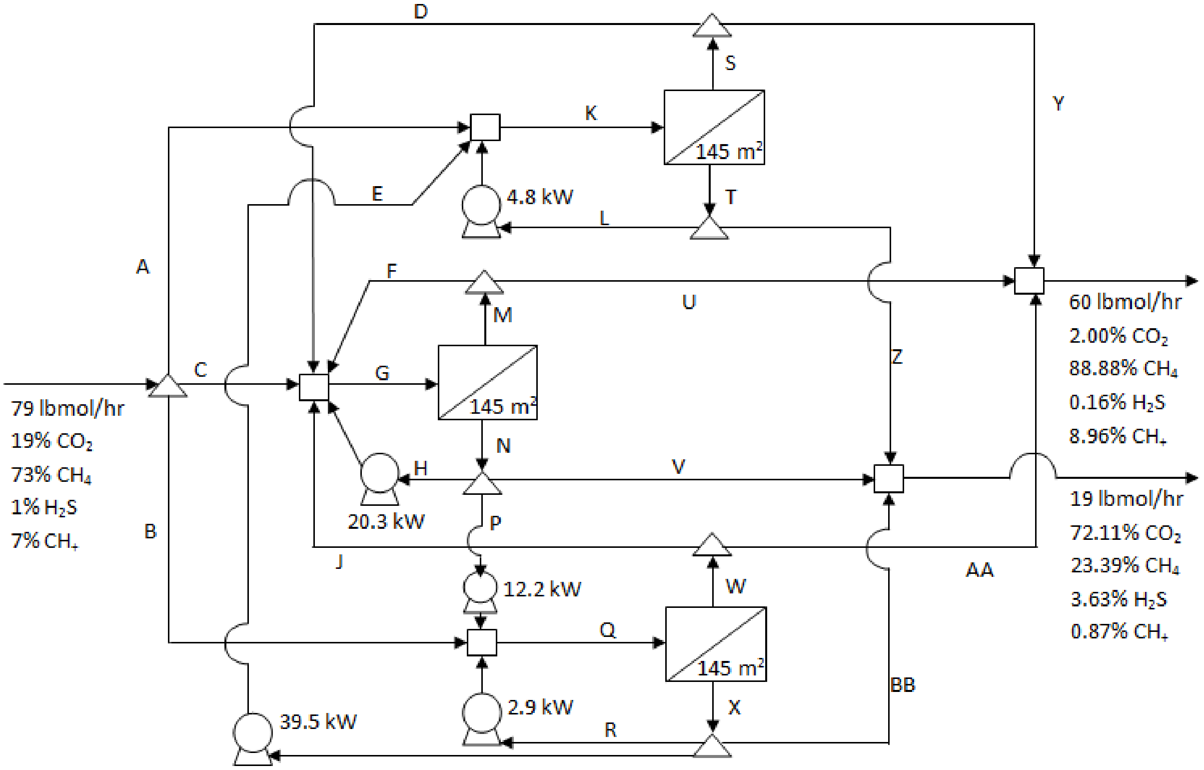

Figure 25. Three membrane network at 79 lb-mol/hr with 19% CO_2

Table 14. Three membrane network molar compositions at 79 lb-mol/hr with 19% CO_2

	A	B	C	D	E	F	G	H	J	K	L	M	N
Flow rate (lbmol/hr)	27.08	42.54	9.73	21.68	14.25	0.14	69.18	6.15	31.48	42.64	1.31	59.30	9.87
% CO2	18.99	19.01	19.00	1.43	63.12	1.93	7.78	42.45	1.94	35.37	72.12	2.01	42.44
% CH4	73.01	73.02	73.00	89.79	32.37	85.14	83.75	53.03	88.88	57.91	23.03	88.87	53.05
% H2S	1.00	1.01	0.98	0.15	3.23	1.57	0.48	2.45	0.18	1.82	3.64	0.16	2.41
% CH+	7.00	6.96	7.01	8.64	1.28	11.35	7.99	2.06	9.00	4.90	1.21	8.97	2.09
	P	Q	R	S	T	U	V	W	X	Y	Z	AA	BB
Flow rate (lbmol/hr)	3.69	47.31	1.06	22.18	20.44	59.18	0.04	31.94	15.37	0.52	19.13	0.45	0.07
% CO2	42.37	21.83	63.43	1.40	72.24	2.01	38.35	1.96	63.12	1.40	72.24	1.78	59.85
% CH4	53.12	70.53	32.09	89.84	23.29	88.85	57.53	88.87	32.44	89.22	23.32	89.13	35.91
% H2S	2.37	1.16	2.99	0.14	3.61	0.16	2.21	0.17	3.20	0.15	3.61	0.18	3.04
% CH+	2.15	6.49	1.49	8.62	0.85	8.97	1.92	8.99	1.24	9.23	0.83	8.91	1.20

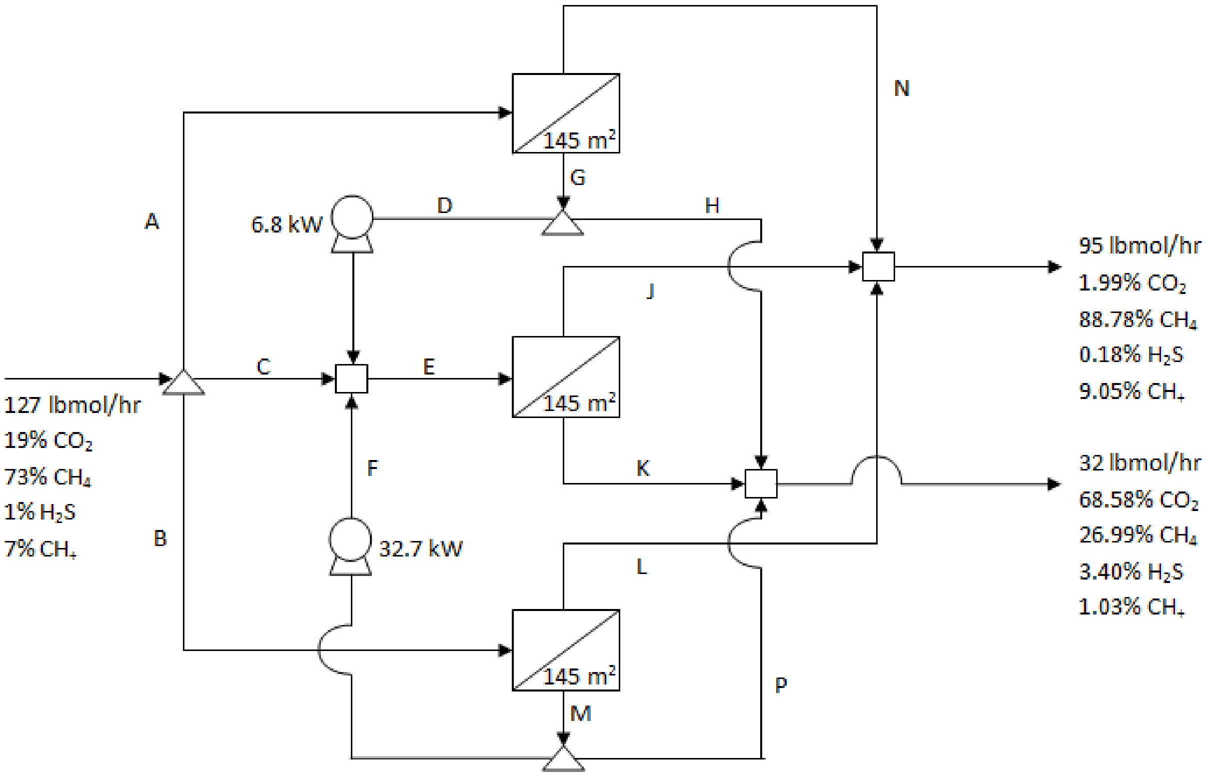

Figure 26. Three membrane network at 127 lb-mol/hr with 19% CO_2

Table 15. Three membrane network molar compositions at 127 lb-mol/hr with 19% CO_2

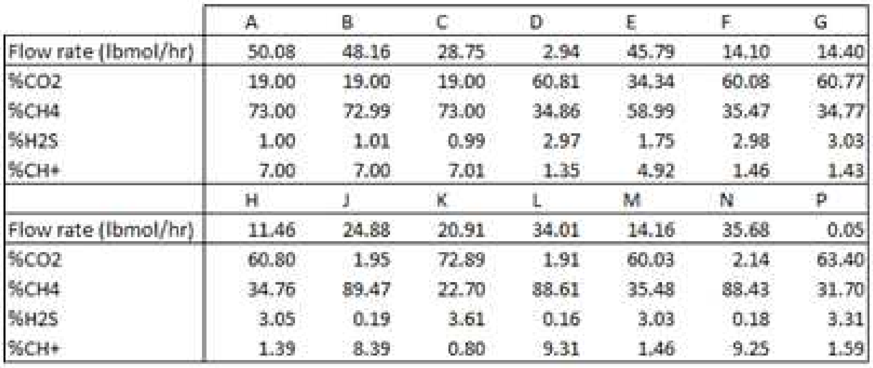

	A	B	C	D	E	F	G
Flow rate (lbmol/hr)	50.08	48.16	28.75	2.94	45.79	14.10	14.40
%CO2	19.00	19.00	19.00	60.81	34.34	60.08	60.77
%CH4	73.00	72.99	73.00	34.86	58.99	35.47	34.77
%H2S	1.00	1.01	0.99	2.97	1.75	2.98	3.03
%CH+	7.00	7.00	7.01	1.35	4.92	1.46	1.43
	H	J	K	L	M	N	P
Flow rate (lbmol/hr)	11.46	24.88	20.91	34.01	14.16	35.68	0.05
%CO2	60.80	1.95	72.89	1.91	60.03	2.14	63.40
%CH4	34.76	89.47	22.70	88.61	35.48	88.43	31.70
%H2S	3.05	0.19	3.61	0.16	3.03	0.18	3.31
%CH+	1.39	8.39	0.80	9.31	1.46	9.25	1.59

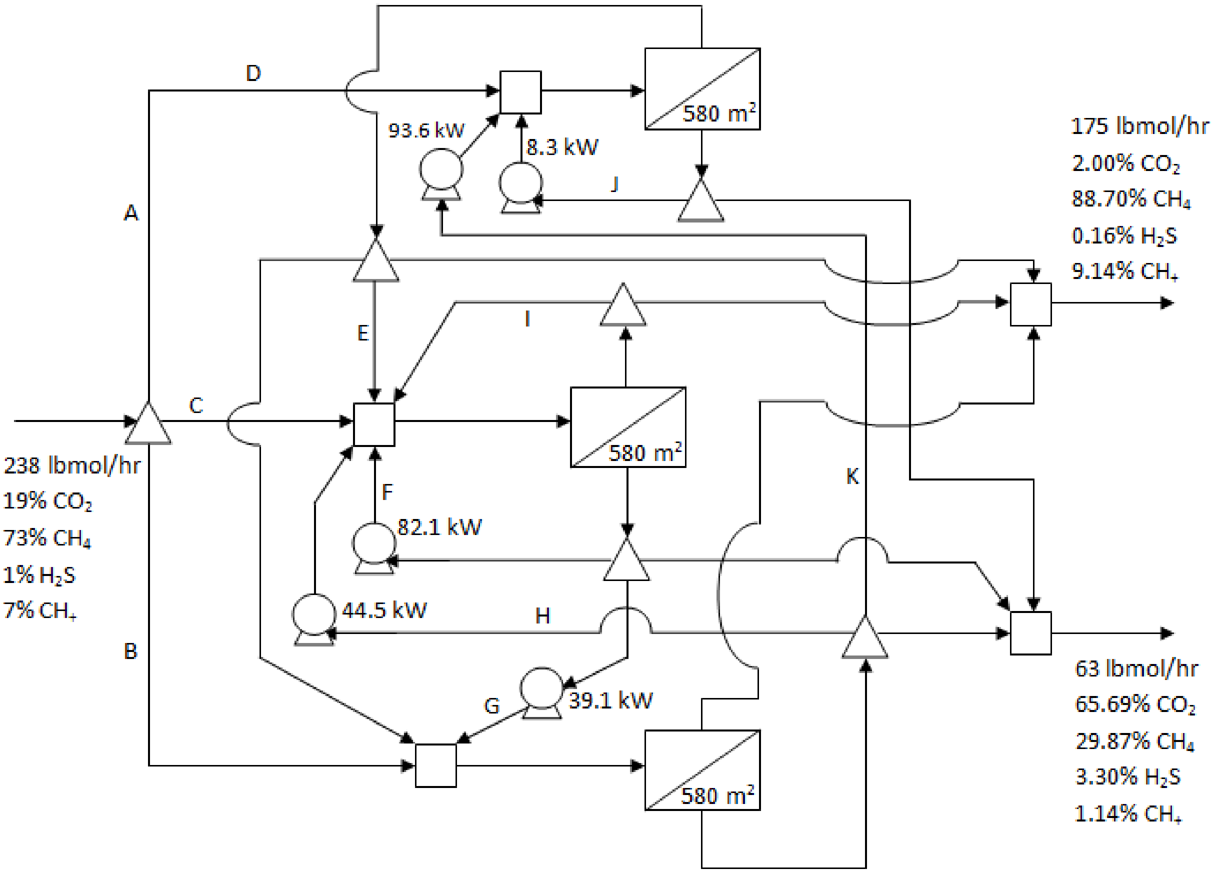

Figure 27. Three membrane network at 238 lb-mol/hr with 19% CO_2

Table 16. Three membrane network molar compositions at 238 lb-mol/hr with 19% CO_2

	A	B	C	D	E	F	G	H	I	J	K
Flow rate (lbmol/hr)	140.68	96.91	0.52	107.91	0.96	31.85	15.18	15.01	171.54	2.68	32.18
% CO2	19.00	19.00	18.28	1.62	1.65	51.91	51.91	52.04	1.99	65.10	52.05
% CH4	73.00	73.00	73.11	89.37	89.12	43.66	43.65	43.52	88.68	29.62	43.51
% H2S	1.00	1.00	1.00	0.15	0.16	2.67	2.67	2.70	0.16	3.23	2.69
% CH+	7.00	7.00	7.62	8.86	9.08	1.77	1.78	1.75	9.17	2.05	1.75

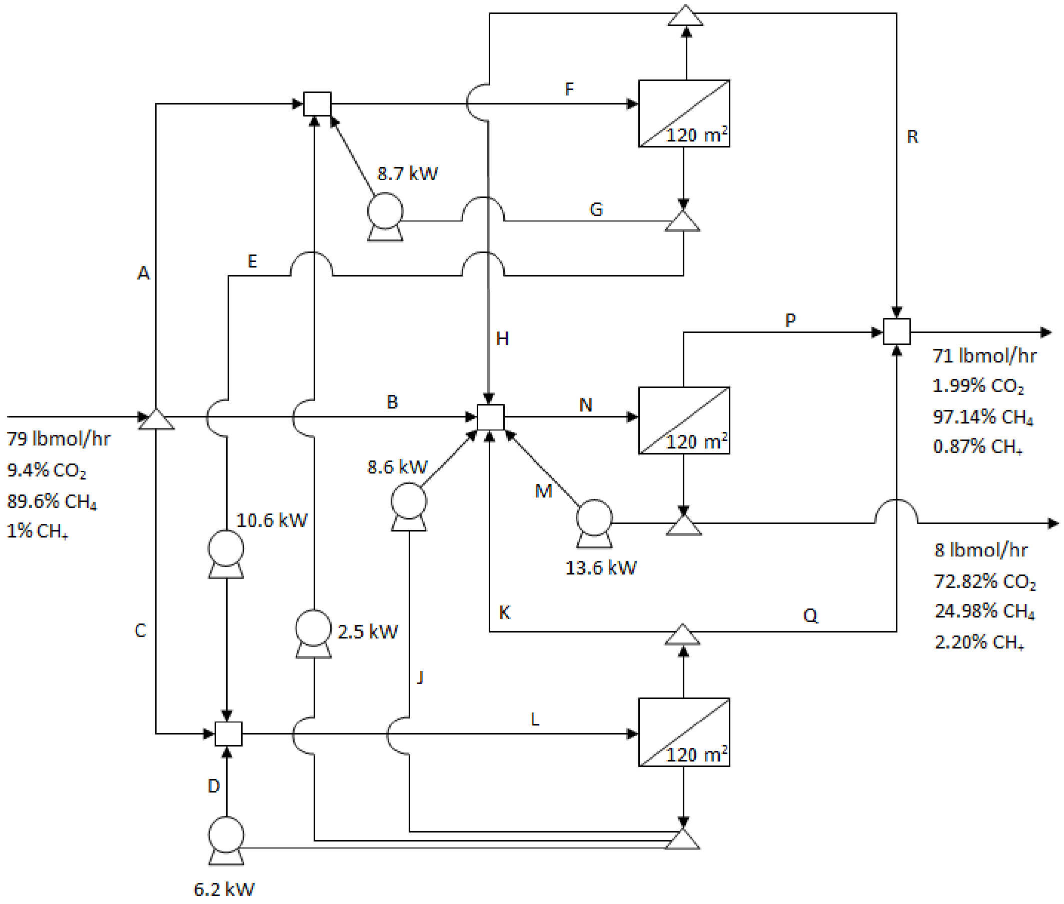

Figure 28. Three membrane network at 79 lb-mol/hr with 9% CO_2

Table 17. Three membrane network molar compositions at 79 lb-mol/hr with 9% CO_2

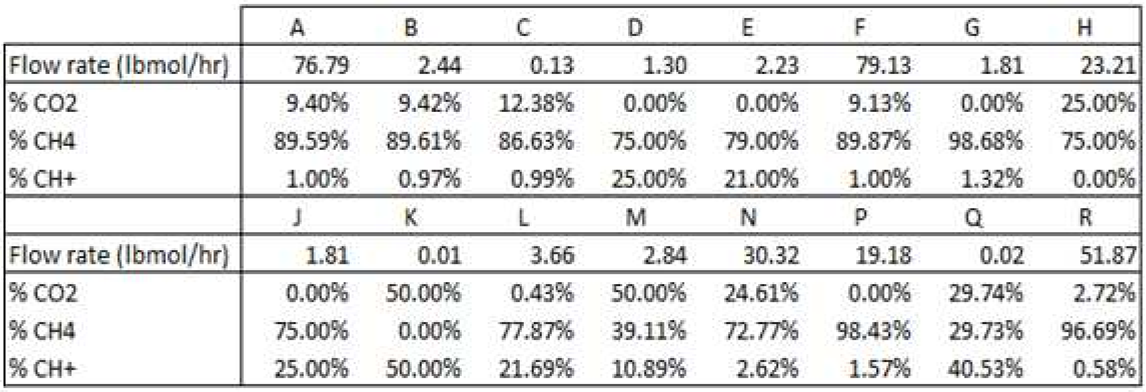

	A	B	C	D	E	F	G	H
Flow rate (lbmol/hr)	76.79	2.44	0.13	1.30	2.23	79.13	1.81	23.21
% CO2	9.40%	9.42%	12.38%	0.00%	0.00%	9.13%	0.00%	25.00%
% CH4	89.59%	89.61%	86.63%	75.00%	79.00%	89.87%	98.68%	75.00%
% CH+	1.00%	0.97%	0.99%	25.00%	21.00%	1.00%	1.32%	0.00%
	J	K	L	M	N	P	Q	R
Flow rate (lbmol/hr)	1.81	0.01	3.66	2.84	30.32	19.18	0.02	51.87
% CO2	0.00%	50.00%	0.43%	50.00%	24.61%	0.00%	29.74%	2.72%
% CH4	75.00%	0.00%	77.87%	39.11%	72.77%	98.43%	29.73%	96.69%
% CH+	25.00%	50.00%	21.69%	10.89%	2.62%	1.57%	40.53%	0.58%